THE MESSENGER

EL MENSAJERO

ESO

Munich

La Silla
La Serena
Santiago

No. 42 – December 1985

FRANK MIDDELBURG 1936–1985

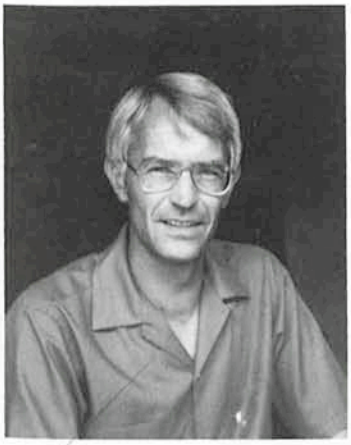

The news of the departure, on November 15, 1985, of Frank Middelburg afflicted the world of astronomy with a special feeling of sadness. Not only was Frank an extremely well-known expert in the field of image processing and a highly respected software system designer, but also a deeply appreciated friend and colleague.

Born on October 8, 1936, in Hong Kong as the son of an ambassador, Frank early became acquainted with an international environment. Newly married to Anita, he joined ESO in 1967 as one of its first European staff members in Chile. The experience he gained at La Silla, first in meteorology and then as an observer, was to become of great value in his subsequent career.

When the first computers came to ESO-Chile, Frank developed into the primary local software expert. He rapidly learned to master not only the computer systems available, but also some of the techniques of image processing, at that time virtually unknown to most people. It was also as an image-processing expert that he left Chile to work at the ESO headquarters, first in Geneva, later in Garching.

Since the beginning of the seventies, software techniques optimized for reduction and analysis of images of celestial objects have been of crucial importance to the explosive development of astrophysics. All over the world, groups of specialists have devoted large amounts of time and effort to improve these techniques.

Frank did it all alone. With a superb grasp of priorities, he designed a versatile and powerful software system with special emphasis on spectral images. The results of Frank's efforts were truly impressive. His Image Handling Programme (IHAP) is still unrivalled for analysis of observations in stellar spectroscopy. At the same time as numerous other software image-processing systems appeared and disappeared, Frank steadily improved the potential of his IHAP. It was a sign of his success that he received so many requests from institutes and individuals to solve also their often quite special problems. A proof of Frank's ability and capacity as well as of his generosity was the fact that he did, indeed, solve virtually all of these problems.

Today, about 15 major institutes have implemented IHAP. Many more institutes dream of having it available, dreams barred by hardware incompatibilities. Currently, the further distribution of IHAP facilities is accelerated through its incorporation into the ESO MIDAS system.

It is difficult to overestimate the importance of Frank's contributions to the European output of astronomical spectrographic data. A large proportion of leading scientists have depended and still depend on the achievements of a single software designer, using IHAP to convert their observations into physically meaningful data.

Those of us who shared the privilege of closer friendship ties with Frank's family also share a common memory of the stimulating atmosphere typical of their home. We will always remember our discussions concerning literature, art, music, politics and other subjects dealt with in the special Middelburg way. Our deep sympathy goes to Anita, Saskia and Miriam, who gave our friend Frank such wonderful support through his difficult last years. Fully aware of how little we can do to console them in their deep loss, we can only assure them that the memory of Frank will be with us forever.

A. ARDEBERG

Automatic Analysis of Interferograms

B. PIRENNE, University of Namur, Belgium; D. PONZ and H. DEKKER, ESO

1. Introduction

Interferometric techniques have been used in optical testing for a long time. The introduction of the laser made this method a routine procedure in the evaluation of the quality of optical components. The interpretation of interferograms is in principle very simple. The fringes represent lines of equal phase difference between two wavefronts, one of which is often flat or spherical. The height difference between two adjacent fringes is usually one wavelength of the radiation used. From the shape and relative order number of the fringes, the map representing the phase difference between the two wavefronts can be reconstructed. Using this phase map, one can then proceed to calculate the more meaningful physical quantities like refractive index variation, distance or stress. This modelling process is different for each application. At ESO, interferometry is used in the testing of optical components for instruments, and programs have been developed that fit the phase map to a set of orthogonal quasi-Zernike eigenfunctions, representing the well-known optical aberrations like spherical aberration or coma. A difficulty has always been to enter into the computer the positions and order numbers of the fringes; up to now this was done manually.

This paper briefly describes a new method of fringe analysis that reduces the manual interaction to a minimum, a more detailed explanation will be given in a forthcoming article.

2. The Method

The method consists of two main steps:
- Fringe detection
- Fringe identification and numbering

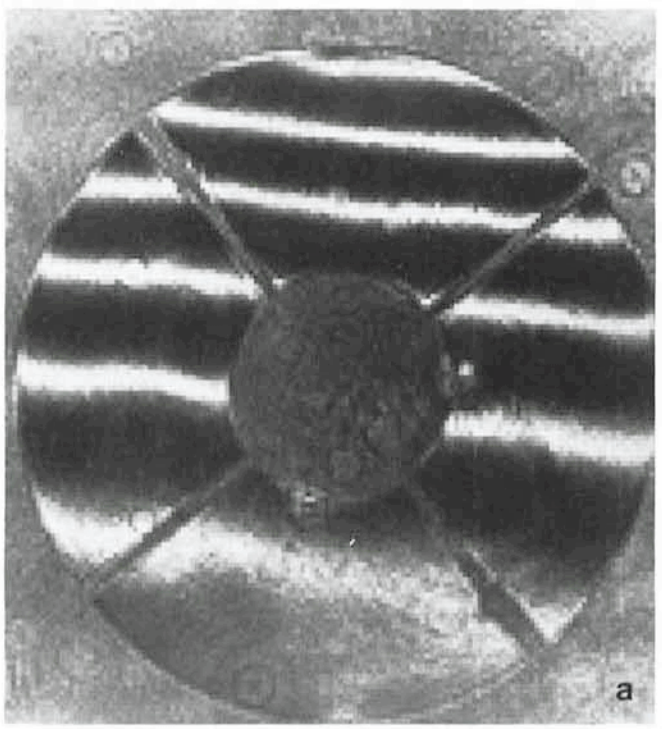

Fig. 1: *Illustration of the method. The original interferogram is shown in 1.a. The detected positions of the fringe maxima are shown in 1.b. In figure 1.c, these positions are connected by the fringe identification algorithm. In the present status of the program, only one link had to be established manually.*

The first step produces, from the original interferogram, a binary image containing information about the positions of the fringe maxima. The value of a pixel in the binary image is 1 if the pixel corresponds to a relative maximum in the original interferogram, and is 0 otherwise.

In the ideal case of a perfect interferogram, this step will be enough to analyse the fringes, and automatic methods proposed so far stop at this stage, perhaps adding a more or less complicated scheme for the numbering of the fringes. However, in real interferograms, the binary image resulting from this step contains disconnected fringe segments, with many spurious positions that were considered as fringes by the algorithm. This is the reason why the available methods do

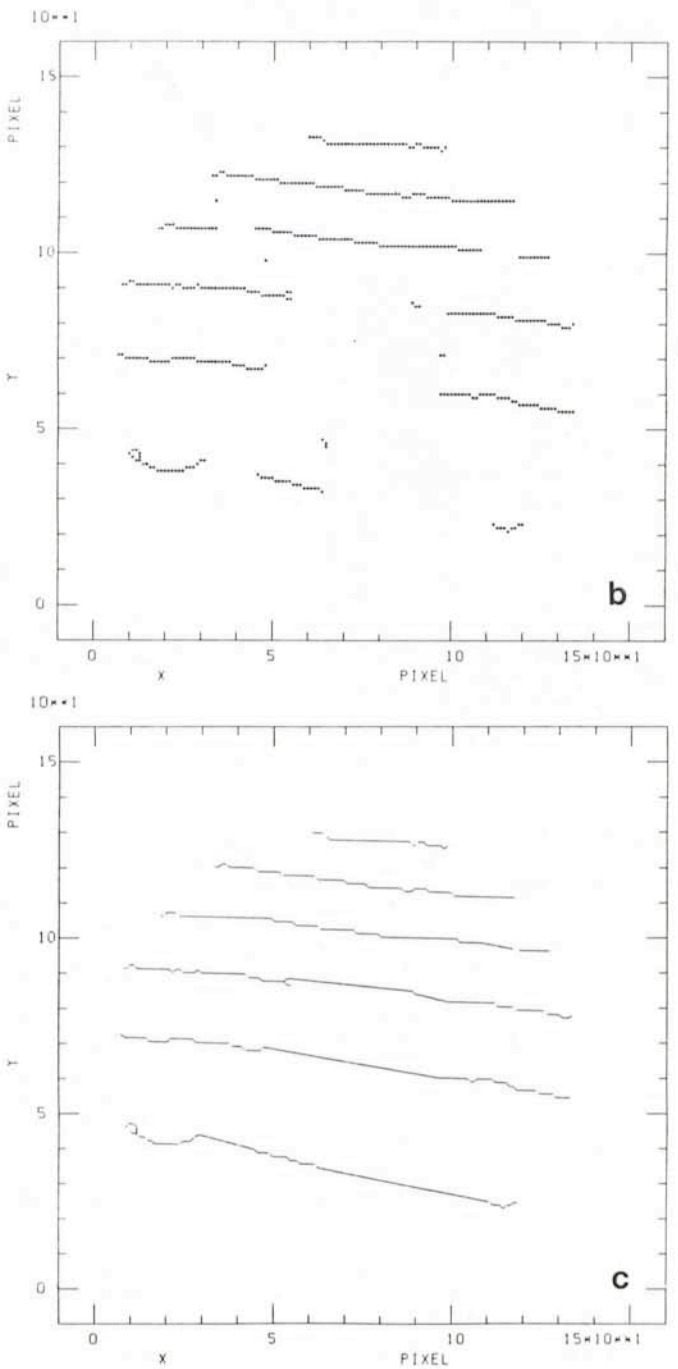

require a substantial interaction to define the numbering of the fringes.

Our method includes a second step where we introduce the information about general properties of fringes (being lines of equal phase), namely: (1) fringes do not intersect, and (2) fringes do not end inside the field of view unless they are circular. By introducing this information we have been able to define an algorithm that "recognizes" the fringes, i.e. is able to reject spurious positions and false fringes, and connects segments belonging to the same fringe. After this step the problem of numbering the fringes is almost trivial and can be done fully automatically.

Given the modularity of the implementation, it is possible to use optional steps to improve the results at any stage in the analysis. The original image can be resampled in order to reduce the image size and the computing time; different filters can be used to reduce the noise in the original interferogram; thinning algorithms will allow a better definition of the fringes in the binary image, previously to the second step.

3. Results

We are testing the method on a large sample of interferograms from which we selected one example in order to illustrate the algorithm; it is a complicated case because some fringes are cut due to the presence of an object in the field of view, and the signal-to-noise ratio is not very good. The results of the method are shown in figure 1. The image in 1.a is the original interferogram; 1.b is a diagram of the positions detected in the first step of the method, it includes spurious fringe positions and shows several fringe segments; finally, figure 1.c is the resulting interferogram, where the spurious fringes are rejected and the true fringes do obey the rules defined in the previous section.

This approach can be used not only for analysis of interferograms; similar principles are applicable to the reduction of multiple object spectra (EFOSC, OPTOPUS) and echelle spectra (CASPEC).

The method has been implemented in MIDAS as a set of commands that allow the automatic analysis of the interferograms as well as the representation of the intermediate results. This implementation opens a new field of applications, so that MIDAS can be used not only for data reduction but also in the testing and integration of new instruments.

4. Acknowledgements

One of us (B.P.) would like to thank ESO for the support through a student position during the duration of this work. We want to express our acknowledgement to F. Merkle and F. Murtagh for helpful discussions and suggestions.

List of ESO Preprints (September–November 1985)

391. F. Matteucci and L. Greggio: On the Relative Role of Type I and II Supernovae and Galactic Chemical Enrichment. *Astronomy and Astrophysics.* September 1985.
392. G. Contopoulos and P. Grosbøl: Stellar Dynamics of Spiral Galaxies: Nonlinear Effects at the 4/1 Resonance. *Astronomy and Astrophysics.* September 1985.
393. M.M. Phillips, C.R. Jenkins, M.A. Dopita, E.M. Sadler and L. Binette: Ionized Gas in Elliptical and SO Galaxies. I. A Survey for Hα and [NII] Emission. *Astronomical Journal.* September 1985.
394. L.B. Lucy, J.A. Robertson and C.M. Sharp: Hayashi Limits for Carbon Stars and the Onset of Dust-Driven Winds. *Astronomy and Astrophysics.* September 1985.
395. G. Contopoulos: Instabilities in Hamiltonian Systems of 2 and 3 Degrees of Freedom. *Particle Accelerators.* September 1985.
396. R.E. de Souza, G. Chincarini and G. Vettolani: Luminosity Function and Morphology-Density Relation. *Astronomy and Astrophysics.* October 1985.
397. O. Stahl and B. Wolf: New Observational Results of the LMC-S Dor Variable R 127 During Outburst. *Astronomy and Astrophysics.* October 1985.
398. E. Brinks and U. Klein: VLA Continuum and HI Observations of Blue Compact Dwarf Galaxies. Contribution to the Proceedings of the Paris Workshop on "Dwarf Galaxies", 1–3 July 1985. October 1985.
399. G. Garay, L.F. Rodriguez and J.H. van Gorkom: Rotating and Expanding Ultra-Compact HII Regions. *Astrophysical Journal.* October 1985.
400. M. Aurière, A. Maucherat, J.-P. Cordoni, B. Fort and J.P. Picat: The X-ray Source in M 15: A Binary Composed of a Neutron Star plus a Post Main-Sequence Star? *Astronomy and Astrophysics.* November 1985.
401. J. Bouvier, C. Bertout and P. Bouchet: DN Tauri, a Spotted T Tauri Star. *Astronomy and Astrophysics.* November 1985.
402. L.N. da Costa, M.A. Nunes, P.S. Pellegrini, C. Willmer, G. Chincarini and J.J. Cowan: Redshift Observations in the Centaurus-Hydra Supercluster Region, I. *Astronomical Journal.* November 1985.
403. E. Oliva and A.F.M. Moorwood: Infrared Objects Near H_2O Masers in Regions of Active Star Formation. IV) Molecular Hydrogen Observations. *Astronomy and Astrophysics.* November 1985.
404. D.L. Lambert and A.C. Danks: On the CH^+ Ion in Diffuse Interstellar Clouds. *Astrophysical Journal.* November 1985.
405. F.-J. Zickgraf, B. Wolf, O. Stahl, C. Leitherer and I. Appenzeller: B[e]-Stars of the Magellanic Clouds. *Astronomy and Astrophysics.* November 1985.
406. B.E. Westerlund, M. Azzopardi and J. Breysacher: Carbon Stars in the Small Magellanic Cloud: I. The Survey Technique and Results for Two Fields. *Astronomy and Astrophysics, Suppl.* November 1985.

A Photometric Study of the Bright Cloud B in Sagittarius: IV. 17 New Diffuse Objects

A. TERZAN, Observatoire de Lyon, France

In 1976, we started a photometric study of the bright cloud B in Sagittarius in the direction of the galactic centre (*The Messenger* No. 10, September 1977).

Since then, our work has been greatly enriched by systematically surveying a large number of U, B, V, R plates, taken by H.E. Schuster and his collaborators with the 1 m Schmidt telescope, and the photometric measurement of several hundred stars with the 1 m and 61 cm Bochum telescopes at La Silla, Chile (Terzan and Bernard, 1981).

We have detected so far:

- 24 diffuse objects: 3 of which are planetary nebulae (Nos. 14, 18, 21); 2 possible globular clusters (Nos. 5 and 23) which are situated in, or projected within, the error boxes of X-ray sources 17065-273 and 17437-316; 1 possible galactic open cluster (No. 20) (Terzan et al., 1978a, b; Terzan and Bernard, 1978; Terzan and Ju, 1980).
- 621 red variable stars (Terzan et al., 1982).
- 42 proper-motion stars (Terzan et al., 1980).

After recently completing our blink survey of all U, B, V, R plates taken for field No. 4 (located south-east of 45 Oph; see *The Messenger* No. 10, September 1977), our list of peculiar objects has lengthened: 567 new red variables have been discovered and 175 stars with annual proper motion larger than 0".2 have been observed.

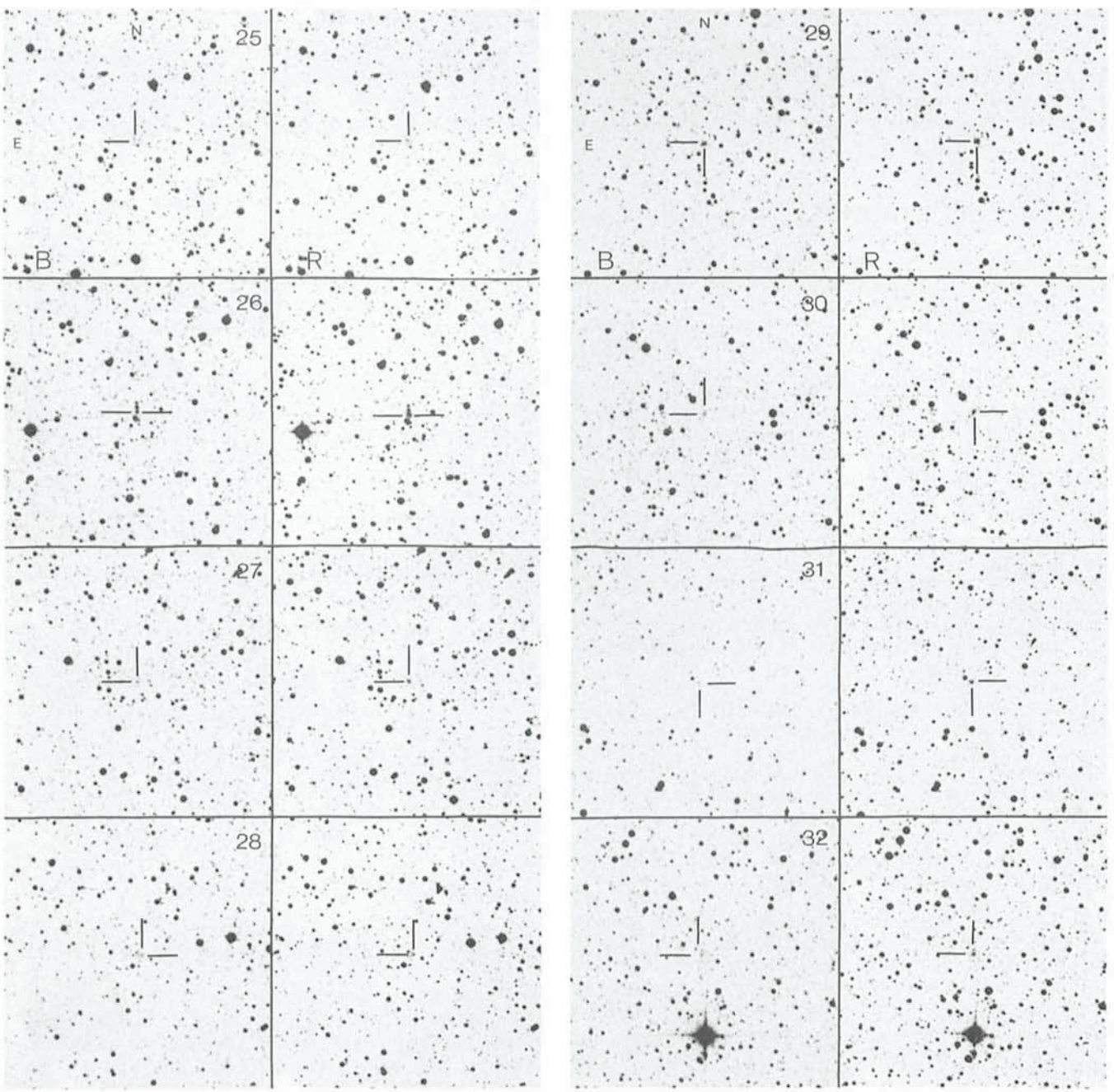

Figs. 1–4: *Finding charts for objects Terzan 25–41, reproduced from the Blue and Red ESO/Schmidt plates. North is at top, east to the left.*

A catalogue, with parameters: α; δ (1950.0), l; b, m_B, m_R, m_{max}, m_{min}, A_{obs} (observed amplitude for variable stars), μ''; $\theta°$ (for proper-motion stars) and an atlas with identification charts – essential for the publication of these results – are under preparation.

Our current research is concentrated on field No. 1 (located north-east of 45 Oph) where, after having blinked the first two pairs of R plates, we have just discovered several hundred other red variables. Their confirmation, however, requires further study of at least other couples of plates.

Also, during the analysis of these 2 first pairs of R plates and 1 pair of B plates, we found 17 new diffuse objects.

Galactic and equatorial coordinates (1950.0) and their X; Y (in mm) positions on the Palomar Observatory Sky Survey (POSS) of these 17 new diffuse objects are given in Table 1. The identification charts–B and R–are reproduced as figures 1–4. We unfortunately do not have a photometric sequence for faint objects ($m_B > 19$ mag; $m_R > 17.5$ mag) within this field, therefore we cannot estimate their m_B and m_R.

Thorough search in the literature and different catalogues leads us to conclude that none of these 17 diffuse objects have been described or catalogued, either as planetary nebulae (Acker, 1985) or known galaxies (Paturel, 1985) nor among van den Bergh's uniform survey of clusters in this area of the southern Milky Way (van den Bergh and Hagen, 1975).

However, it should be pointed out that Johnston et al. (1981), during their search for an optical counterpart of the extended X-ray source detected with the HEAO 1 Scanning Modulation Collimator near 4U1708-23 ($l = 0\overset{\circ}{.}5$; $b = 9\overset{\circ}{.}4$), found an anonymous $z = 0.03$ cluster of galaxies (CL 1709-233), Ophiuchus Cluster) which falls outside the northern limit of our field, subject of the present paper.

Within a $2\overset{\circ}{.}1 \times 2\overset{\circ}{.}6$ rectangle centered on their so-called "dominant central galaxy" ($17^h09^m25\overset{s}{.}6$; $-23°18'35''$, 1950.0) Johnston et al. have found 108 galaxies and they suggest that the steep-spectrum radio source MSH 17-023 is associated with this cluster.

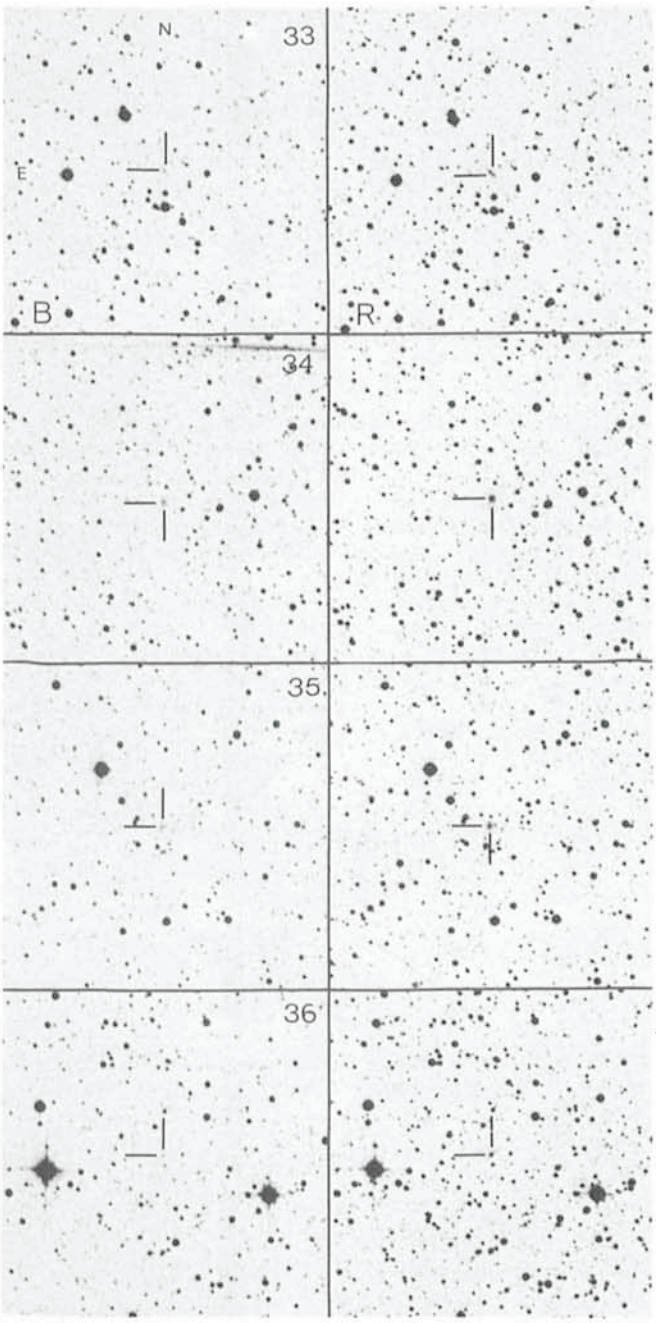

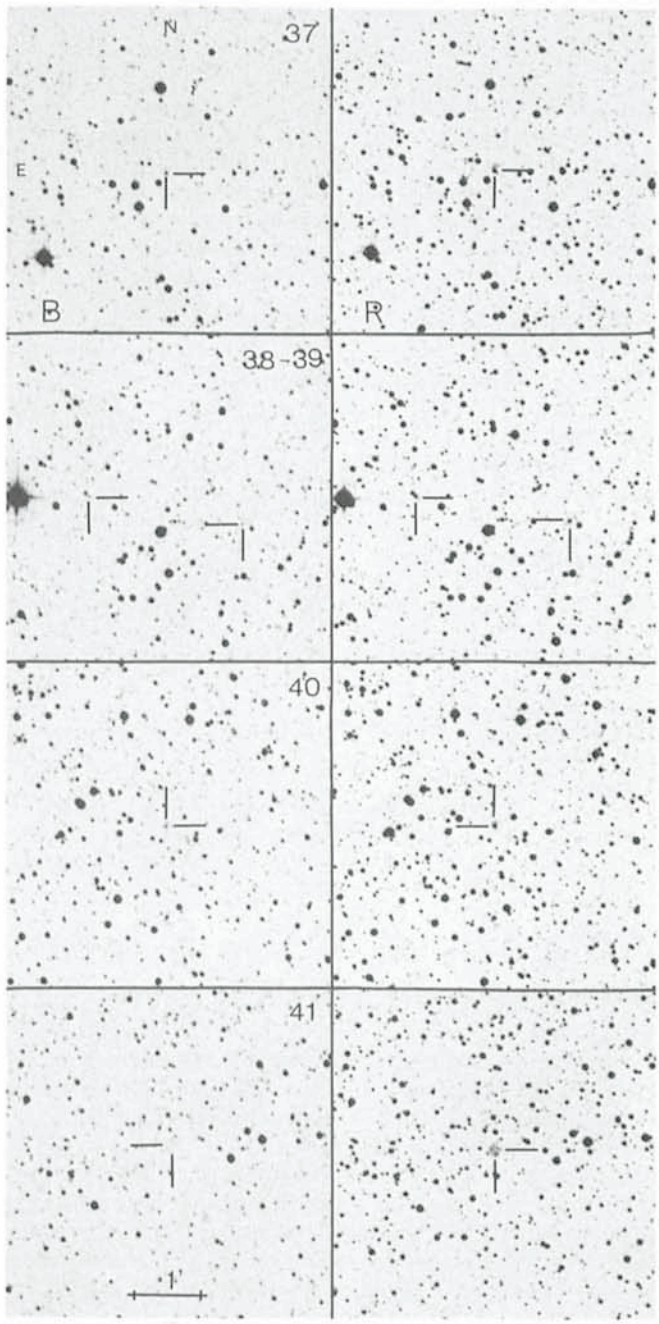

All charts have the same scale.

TABLE 1

Object (Terzan No.)	(1950.0)		POSS		
	α	δ	Charts	X_{mm}	Y_{mm}
25	$17^h03^m08^s.5$	$-24°46'44''.6$	$-24°\ 16^h54^m$	117.6	139.4
26	$17^h04^m41^s.4$	$-24°59'47''.4$	$-24°\ 16^h54^m$	99.0	127.5
27	$17^h04^m52^s.6$	$-24°48'30''.1$	$-24°\ 16^h54^m$	96.5	137.6
28	$17^h05^m04^s.1$	$-25°15'03''.0$	$-24°\ 16^h54^m$	94.5	113.7
29	$17^h05^m15^s.4$	$-25°09'51''.3$	$-24°\ 16^h54^m$	92.2	118.2
30	$17^h06^m09^s.6$	$-24°55'21''.1$	$-24°\ 16^h54^m$	81.0	131.2
31	$17^h08^m20^s.2$	$-24°52'10''.5$	$-24°\ 16^h54^m$	54.2	135.7
32	$17^h09^m27^s.2$	$-25°08'34''.7$	$-24°\ 16^h54^m$	41.4	118.8
33	$17^h09^m31^s.9$	$-25°03'10''.8$	$-24°\ 16^h54^m$	40.5	123.4
34	$17^h10^m11^s.2$	$-24°58'58''.0$	$-24°\ 16^h54^m$	32.3	127.0
35	$17^h10^m57^s.6$	$-24°45'30''.2$	$-24°\ 16^h54^m$	23.0	138.8
36	$17^h12^m31^s.1$	$-24°55'40''.7$	$-24°\ 17^h20^m$	316.0	126.3
37	$17^h12^m35^s.5$	$-25°15'55''.9$	$-24°\ 17^h20^m$	315.0	108.5
38	$17^h13^m03^s.9$	$-24°55'53''.3$	$-24°\ 17^h20^m$	309.5	126.3
39	$17^h13^m13^s.9$	$-24°55'42''.4$	$-24°\ 17^h20^m$	307.8	126.5
40	$17^h13^m42^s.5$	$-24°55'55''.9$	$-24°\ 17^h20^m$	302.0	126.5
41	$17^h17^m17^s.9$	$-24°48'53''.8$	$-24°\ 17^h20^m$	258.8	134.0

It is highly probable that some of our 17 diffuse objects are galaxies belonging to this cluster.

At any rate, none of the descriptions or hypotheses (globular cluster, planetary nebula, galaxy, star surrounded by nebulosity) given under "Description of Objects" should be regarded as definite. They can only help toward future talks based on deeper studies (photometry, spectrophotometry) which we propose to undertake later on with a large telescope.

Addenda: After writing the above paper (May 1985) we have found other diffuse objects, quite close to this Ophiuchus Cluster. This fact leads us to believe that:

1. The total number of galaxies belonging to this cluster must be clearly in excess of 108;

2. The entire cluster must actually extend far beyond a $2.^\circ1 \times 2.^\circ6$ field.

Description of Objects

Terzan 25 – nebulosity, surrounding a center, well defined on the R plates
Terzan 26 – planetary nebula?
Terzan 27 – nucleus of galaxy or a star surrounded by nebulosity
Terzan 28 – nebulosity
Terzan 29 – planetary nebula or a red star surrounded by nebulosity
Terzan 30 – galaxy?
Terzan 31 – galaxy?
Terzan 32 – probably a spiral galaxy judging from B plates
Terzan 33 – center of a globular cluster? nebulosity is evenly distributed on R plates
Terzan 34 – probably a globular cluster with a strong central concentration on R plates
Terzan 35 – globular cluster or planetary nebula?
Terzan 36 – nucleus of galaxy?
Terzan 37 – nebulosity
Terzan 38 – nucleus of galaxy or a star surrounded by an elongated nebulosity
Terzan 39 – galaxy?
Terzan 40 – planetary nebula?
Terzan 41 – nebulosity of an almost spherical form

References

Acker, A., 1985, Private Communication.
van den Bergh, S. and Hagen, L., 1975, *Astronomical Journal,* **80.**
Johnston, M.D., Bradt, H.V., Doxsey, R.E., Margon, B., Marshall, F.E. and Schwartz, D.A., 1981, *Astrophysical Journal,* **245.**
Paturel, G., Private Communication.
Terzan, A., Bernard, A. et Ju, K.H., 1978a, Comptes Rendus Acad. Sciences, Paris, **287,** serie B, 157.
Terzan, A., Bernard, A. et Ju, K.H., 1978b, Comptes Rendus Acad. Sciences, Paris, **287,** serie, B, 235.
Terzan, A. and Bernard, A., 1978, *The Messenger,* **15.**
Terzan, A., and Ju, K.H., 1980, *The Messenger,* **20.**
Terzan, A., Bernard, A., Fresneau, A. et Ju, H.K., 1980, Comptes Rendus Acad. Sciences, Paris, **290,** serie B, 321.
Terzan, A. and Bernard, A., 1981, *Astronomy and Astrophysics, Suppl. Series,* **46.**
Terzan, A., Bijaoui, A., Ju, H.K. and Ounnas, Ch., 1982, *Astronomy and Astrophysics, Suppl. Series,* **49.**

A Catalogue of Dwarf Galaxies South of $\delta = -17.^\circ5$

J.V. FEITZINGER and TH. GALINSKI, Astronomisches Institut, Ruhr-Universität Bochum

The first systematic search for dwarf galaxies was undertaken by van den Bergh (1959) and resulted in a catalogue which contained 222 objects north of $\delta = -23°$ (in 1966 the list was expanded to 243 dwarfs north of $-33°$). Nilson (1973) noted in his "Uppsala General Catalogue of Galaxies" 687 dwarf systems north of $-2.^\circ5$. Both catalogues were produced with the aid of the "Palomar Observatory Sky Survey". The publication of two photographic surveys of the southern hemisphere ($\delta < -17.^\circ5$), namely the ESO(B) and the SRC(J) Atlas, available in Bochum as plate and film copy respectively, permitted a systematic search for dwarf galaxies in that region.

As a basis for the present survey served the "ESO/Uppsala Catalogue" (Lauberts 1982), from which we chose as possible "dwarf candidates":

- all spiral galaxies which were classified as Sc and later or as S . . .,
- all elliptical galaxies,
- all irregular galaxies,
- all dwarf galaxies,
- all peculiar objects,

as far as their major axis had a minimum of 1′.

It was necessary to reexamine the Lauberts sample, restricted by the dwarf galaxy criteria, since the coarse Lauberts classification based on ESO(B) plates does not record adequately the dwarf galaxy population. But the Lauberts catalogue is still well suited for the purpose of object identification. It is homogeneous and almost complete with respect to objects larger than 1.'0.

We started with a total of 7,002 systems. A final threefold examination led to a catalogue containig 584 systems, from which 20 did not appear in the ESO/Uppsala Catalogue. The catalogue is published in *Astronomy & Astrophysics Supplement Series,* **61,** 503, 1985.

Figure 1 presents the distribution of the 584 dwarf galaxies in Aitoff projection. The belt of the Milky Way is clearly seen, the SMC and LMC are also marked and four pronounced empty regions.

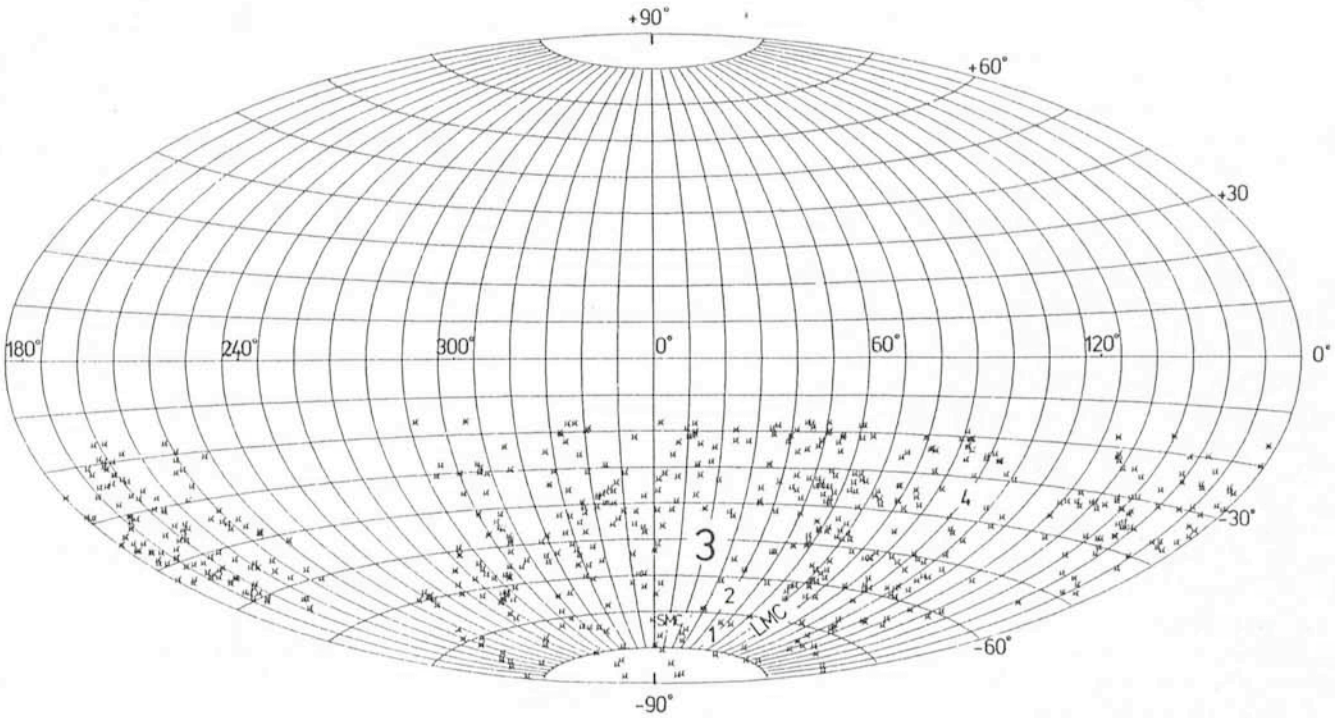

Figure 1: *Distribution of the dwarf galaxies on the sphere in an Aitoff projection. The Milky Way and the Magellanic Clouds as well as four other pronounced empty regions are indicated. The regions (1, 2, 3) coincide with the Magellanic stream, region 4 coincides with a dark cloud complex (No. 445, 446, 447, 450, 453 in the catalogue of Feitzinger and Stüwe, 1984).*

THE EXTRINSIC ABSORPTION SYSTEM IN THE QSO PKS 2128-12:

A Galaxy Halo with a Radius of 65 kpc

J. BERGERON, Institut d'Astrophysique, Paris

1. The Different Types of Extrinsic Absorption Systems

A large number of absorption lines are detected in the spectra of QSOs. Most of them are identified with lines from ions of abundant elements at a redshift z_α smaller than the QSO emission redshift z_Q and their velocity dispersion is small, typically $5 \leq \sigma_v \leq 50$ km s^{-1}. These absorption systems at $z_\alpha < z_Q$ are now commonly believed to be of intervening origin, but their exact nature remains still an open question. Indeed, these systems are only known by their absorptions. Most of them are too faint to be accessible to direct observations with present-day techniques, except, may be, those at small redshift.

Before describing our attempt to detect directly one of the low z absorption systems, let us quickly present the two main classes of extrinsic absorbers, that is those at $z_\alpha < z_Q$. First there are metal-rich systems in which hydrogen and the most abundant heavy elements are present. These absorbers could be associated with galaxies, but then all spiral galaxies must have gaseous halos about four times larger than the luminous parts of the galaxies. This population has been detected within a large redshift range from about 0.2 to 3.7. The high redshift absorption systems, detected mainly by their C IV absorption, have some properties which differ from those of the lower redshift ($z \leq 1$) absorbers, detected up to now by their Mg II or Fe II absorptions (a survey of their C IV absorption would require a large space-based UV telescope). They are much more numerous than the low z systems, even after removing the effect due to the expansion of the universe, and they have a higher degree of ionization. In the assumption of absorption by intervening galaxies, this may suggest that either the degree of ionization of gaseous halos increases outwards, or that these halos were larger and more ionized in the past.

The second population of absorption systems has primordial or very metal-poor gas, with only lines of the H Lyman series present. These absorbers, called the Lyα forest, are known only at $z \geq 1.7$ and their study at smaller z will be done

when a large space-based UV telescope will be available. At z = 2.5, the number density of these systems is one hundred times larger than for the metal-rich population. This raises the crucial problem, not yet solved, of the nature of the Lyα forest systems: do they constitute a primordial population independent of the galaxies? How do they evolve? Has any of these systems survived to the present epoch?

2. Detection of a Galaxy Identified with the Absorption System in PKS 2128-12

Since no extrinsic system at $0.1 < z_\alpha < z_Q$ has yet been identified, we have concentrated our efforts on the most promising cases: the metal-rich absorbers at low redshift. If these systems are associated with extended disks or halos around spiral galaxies, it should be possible to detect these galaxies by broad band imaging. Indeed a typical spiral galaxy at $z \leq 0.5$ should have a magnitude m (V) $\leq$ 22.5 (Weymann et al. 1978, Guiderdoni and Rocca-Volmerange, 1985) within the range of detectability with present-day techniques. The Holmberg diameter (magnitude limit of 25 per arcsec^2) of a typical spiral galaxy is 44 kpc (average over the luminosity function and using H_o = 50 km s^{-1} Mpc^{-1}) or about 6 arcsec at z = 0.5 (independent of H_o). This implies that in good seeing conditions, faint distant galaxies at $z \leq 0.5$ are resolved and therefore can be distinguished from faint foreground Galactic stars. Finally, although the galaxies possibly associated to the absorbers are faint and close on the sky to a bright point source, the QSO, they are not so close as to be undetectable. The average size of the absorbers derived from Mg II statistical studies (Young et al. 1982) corresponds to an angular radius of 6 arcsec at z = 0.5, distance from the QSO large enough to detect a 22-magnitude object close on the sky to a 16 magnitude point source even with moderately good seeing.

We started a CCD broad-band imaging survey of QSOs with low redshift absorption systems and found in 8 cases faint extended objects, less than 15 arcsec away from the QSO line of sight.

A narrow absorption Mg II doublet at z = 0.4299 is present in the spectrum of the QSO PKS 2128-12. The QSO emission redshift is 0.501 and the absorber should belong to the class of extrinsic systems. The field around PKS 21218-12 was first observed during our CCD broad-band imaging survey in September 1982, at the 1.5 m Danish Telescope on La Silla. We discovered a faint object 8.6 arcsec northeast from the QSO, which was resolved in the images of best seeing (resolution: FWHM = 1.3 arcsec) and has a magnitude in the Gunn r band of 21.0.

A spectroscopy follow-up of this faint object, potential candidate for the absorber, became possible with the availability of the ESO faint object spectrograph and camera (EFOSC). In September 1985, we observed at the 3.6 m telescope on La Silla the field around PKS 2128-12 in the imaging mode of EFOSC through a V filter. The exposure time was 3 minutes and the image was corrected from the CCD offset and flatfielded. The 2.9 arcmin square central parts are shown in Fig. 1, and 10 resolved objects are present. The object 8.6 arcsec northeast of the QSO (labelled $\neq$ 1 in Fig. 1) has a magnitude m_v = 21.5. The next closest ($\neq$ 3) is much further away at a distance of 38 arcsec from the QSO line of sight. The spatial distribution of the resolved objects is fairly homogeneous, with no special clustering around the line of sight to the QSO.

In the spectroscopy mode of EFOSC we took two spectra of object $\neq$ 1, each of one hour exposure. A blue grism providing a dispersion of 230 Å per mm was used and the slit width was of 1.5 arcsec. This combination gives a spectral resolution of

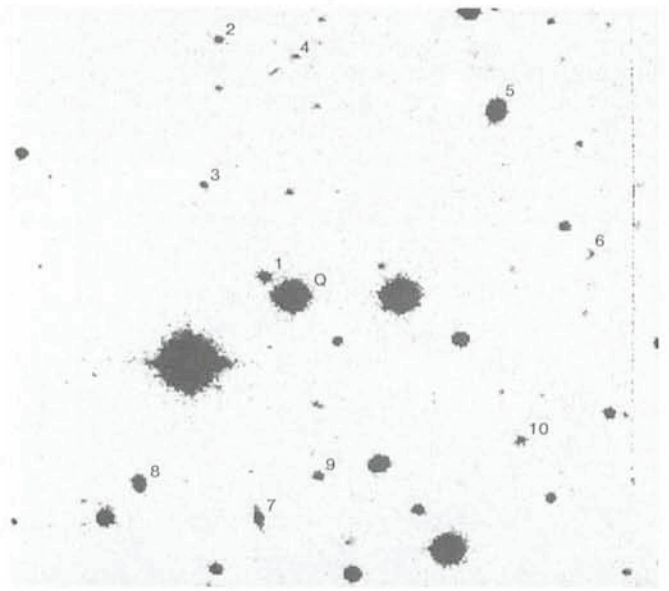

Fig. 1: *CCD imaging with EFOSC at the 3.6 m of the field around the QSO PKS 2128-12. This is a 2.9 arcmin square field centered on the QSO. Northeast is at the top left corner. The seeing is of FWHM = 1.6 arcsec.*

FWHM = 14 Å in the wavelength range $\lambda\lambda$3700–7000. At the blue edge of this region, $\lambda \leq$ 3950 Å, the sensitivity of the RCA CCD used was too low to detect any signal from a faint target as object $\neq$ 1. After each exposure on the object we recorded a flat field image and Helium and Argon spectra. The slit was oriented in the east-west direction and the spectrum of object $\neq$ 1 was integrated over 5 pixels or 3.4 arcsec along the slit. The resulting spectrum is shown in Fig. 2 after sky subtraction and wavelength calibration. The signal to noise ratio reaches 10 to 12 in the central parts of the spectrum.

Two emission lines (one just at the red end of the spectrum) are clearly visible as well as two close-by absorption lines. The continuum and the emission line at λ 5331.7 are resolved along the slit when compared to the spectrum of a standard star. The redshift derived from all the detected lines is z = 0.430 $\pm$ 0.001, value equal to the redshift of the absorption system. The lines present are identified with [OII] λ3727 and Hβ in emission and Ca II H and K in absorption.

3. Nature of the Mg II Absorption System Detected in PKS 2128-12

The z = 0.4299 absorption system in PKS 2128-12 appears to be associated with a gas-rich galaxy with center 8.6 arcsec or 64 kpc away from the QSO line of sight. Within the uncertainty of our measurements, Δv = 210 km s^{-1}, the galaxy and the absorber have the same redshift. The galaxy is elongated in the east-northeast, west-southwest direction and the line of sight of the QSO intercepts the plane of the galaxy at a radius of 80 to 110 kpc, or 4 to 5 Holmberg radii. The projected radius of the visible part of the galaxy (V or Gunn r images) is only of about 15 kpc in the direction towards the QSO line of sight.

Are there other properties of the absorption system which may help to specify the nature of the absorber: disk or halo? The H I column density of the absorber can be derived from UV observations of PKS 2128-12 with IUE (Bergeron and Kunth, 1983). From the existence of a Lyman discontinuity at $z = z_\alpha$, and using a damping limit for Lyα absorption we find $4\ 10^{17} < N\ (H\,I) \leq 8\ 10^{18}$ cm^{-2}. The absorber is optically thick to UV ionizing photons but is not a cloud of neutral gas since Mg is not mainly in the atomic form N (Mg I)/N (Mg II) = 10^{-3} (Tytler et

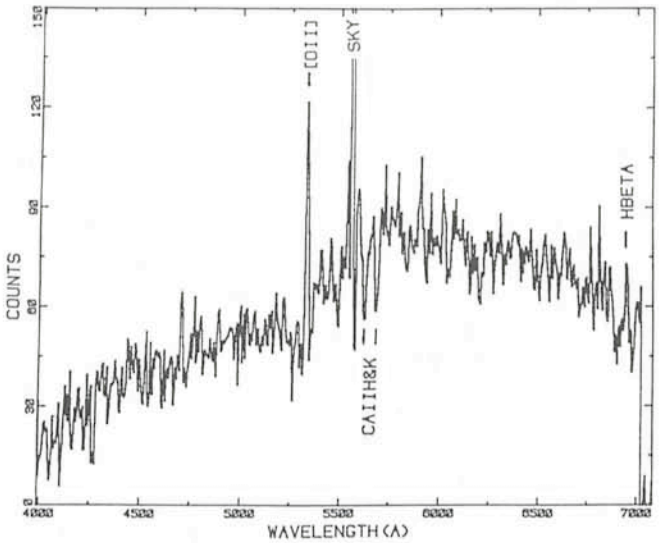

Fig. 2: *Spectrum of galaxy ≠ 1 (m_v = 21.5) 8.6 arcsec northeast of the QSO obtained with EFOSC. It is the sum of two spectra, each of one hour exposure. The spectral resolution is FWHM = 14 Å. The redshift derived from the emission and absorption lines is 0.430; it is equal to the redshift derived from the MgII doublet detected in absorption in the spectrum of the QSO.*

al., 1985). The velocity dispersion of the MgI and MgII lines is small, b ~ 8 km s^{-1}, and the HII column density derived in the assumption of normal abundances is 7 10^{19} cm^{-2} if Mg is mainly singly ionized. The CIV doublet is not detected in the UV spectrum with w (CIV 1549)/w (MgII 2800) ≤ 1.3, and the degree of ionization of the absorber appears similar to, or possibly lower than, those observed in high latitude gas in our Galaxy.

From the above properties we conclude that the absorbing cloud on the line of sight to PKS 2128-12 is more likely associated to a very extended disk than to a halo around a spiral galaxy of absolute luminosity M_V = −20.8.

References

Bergeron, J., Kunth, D.: 1983, *Monthly Notices Roy. Astron. Soc.* **205,** 1053.

Guiderdoni, B., Rocca-Volmerange, B.: 1985, Erice workshop, Spectral evolution of galaxies, in press and pré-publication N°110, Institut d'Astrophysique, Paris.

Tytler, D., Boksenberg, A., Sargent, W.L. W., Young, P., Kunth, D.: 1985, preprint.

Weymann, R.J., Boroson, T.A., Peterson, B.N., Butcher, H.R.: 1978, *Astrophys. J.* **226,** 603.

Young, P., Sargent, W.L.W., Boksenberg, A.: 1982, *Astrophys. J. Suppl.* **48,** 455.

Comet Halley's Plasma Tail Photographed from Germany with a Focal Reducer to be Used at ESO's 1 m Telescope

K. JOCKERS, Max-Planck-Institut für Aeronomie, Katlenburg-Lindau, FRG, and
E. H. GEYER, Observatorium Hoher List, Daun, FRG

A picture of the plasma tail of Comet Halley was obtained at the 1 m telescope of Hoher List Observatory on November 12, 21 UT. A focal reducer, combining instrumentation built at Hoher List Observatory and the Max-Planck-Institute for Aeronomy, was used. At a 1 m telescope the plate scale of the focal reducer very nearly equals the scale of the ESO Schmidt telescope but the field has only 25 mm diameter, corresponding to about 0°.5 in the sky. The exposure of Comet Halley was taken through an interference filter of a bandpass of 425+/−3nm, which transmits the 0–2 band of the CO^+ comet tail band system. A two-stage proximity focus image intensifier was employed and 103a-F film was pressed against its exit window. Exposure time was 15 minutes.

The picture is shown in figure 1. At the time of exposure Comet Halley was at a geocentric distance of 117 million kilometers and quite close to opposition, i.e. the angle earth-comet-sun was only 9°. This is an unusual geometry for comet observations. As the cometary plasma is interacting with the solar wind, which flows nearly radially out of the sun, the comet tail is always pointing away from the sun. Therefore, in the picture we look very much along the cometary tail. While the projected length of the comet tail as seen on the photograph amounts to about 5 × 10^5 km, its true length may exceed 3 million kilometers. The fact that in the picture the tail forms a large angle with the antisolar direction may be caused by a slight deviation of the solar wind direction from radial towards south.

With the same instrumentation a program will be conducted at the ESO 1 m telescope when Comet Halley will be best visible from the southern hemisphere. The program aims at the determination of content and topology of cometary ions CO^+, N_2^+, CO_2^+ and H_2O^+ in relation to the neutral coma molecules. Considering the excellent sky conditions at La Silla as compared to German November days we hope to obtain very good observations in March and April 1986.

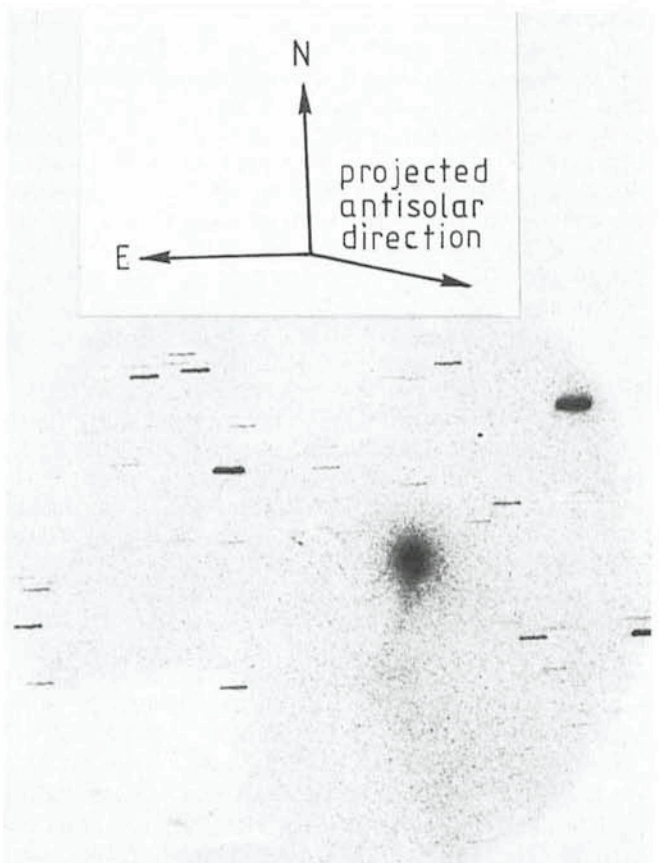

Discovery of Neptune's Ring at La Silla

R. HAEFNER, Universitäts-Sternwarte München,
J. MANFROID, Institut d'Astrophysique Liège, Belgium, and P. BOUCHET, ESO

The story of the discovery of the planet Neptune is well known: During the years 1841 to 1845 the English Cambridge student J.C. Adams calculated the position of an eighth planet based on the difference between the predicted and observed orbit of the planet Uranus, thought to be the outermost one in our solar system. However, J. Challis, at that time Director of the Cambridge Observatory, as well as G.B. Airy, Director of the Greenwich Observatory, refused to point their telescopes toward the calculated position. Challis considered a search to be too troublesome and expected a negative result. Airy, on the other hand, was convinced that the quadratic law of distance had to be changed to obtain the observed Uranus orbit. Independently and roughly at the same time the French astronomer J.J. Leverrier worked on the same problem and published nearly the same position of an eighth planet. He wrote then a letter to the Urania Observatory in Berlin which he thought to be the best one in Europe at that time. Thereupon, in the night of September 23, 1846, J.G. Galle and his assistant H.L. d'Arrest found the eighth planet Neptune in Aquarius just after one hour of comparing the observed star position with those on a star chart they had drawn half a year ago. This was one of the first examples of European astronomical cooperation. To be complete it should be mentioned that Challis after all started observations. He saw the new planet several times prior to Galle, but he did not realize it.

The next story is little known: The English amateur W. Lassell who promptly detected Neptune's satellite Triton at the Starfield Observatory in Liverpool, reported also on the discovery of a ring around Neptune on October 3, 1846 (fig. 1). He saw the "ring" as a diametrical bulge on the planet's disk again on several occasions in November and December 1846, interrupted by bad weather conditions. Lassel's discovery was widely discussed in the London *Times*, the *MNRAS* and the *Astronomische Nachrichten* and later on confirmed by Challis who was now eager to participate on a new detection. However, a comparison of their drawings revealed a different orientation of the suspected ring. Consequently, using the new Harvard refractor in 1847, W.C. Bond of the Cambridge Observatory (Massachusetts) was unable to see the phenomenon and attributed Lasell's finding to an optical appendage with preconception doing the rest. Extensive searching during the second part of the 19th century and the beginning 20th century by means of large refractors of high optical quality was not successful in finding any features which fitted the descriptions given by Lassell and Challis.

It is however interesting to note that after his discovery of Uranus in 1781, F.W. Herschel observed on several occasions during the years 1787 to 1792 a ring around this planet appearing as an elongate appendix on both sides of the planet's disk. Later on this phenomenon disappeared and Herschel was convinced to have been a victim of an optical delusion. However, there are in fact indications that Herschel really saw the ring system: a recalculation of the orientation of the rings detected in 1977 shows an exact agreement with the position given by Herschel; the disappearance can be explained by the edge-on position at that time (Schmeidler, 1985).

Indeed, the unexpected (re)discovery of the Uranian rings during an occultation of a late-type star by the planet in 1977 as well as the discovery of the faint Jovian rings by the Voyager 1 spacecraft in 1979 stimulated the search for such rings around the fourth of the giant planets, Neptune.

The main ground-based technique to establish the existence of faint rings around a distant planet is to follow a stellar occultation, which is one of the most ancient forms of astronomical observations. Using high-speed photometric techniques the intensity of the star light is measured during the passage of the rings through the line of sight which dims the intensity in the order of a few seconds. Such occultations by, and appulses to, interesting planets are predicted and published several years in advance together with information on where and when they will be visible. During the last years there was at least one good opportunity each year as far as Neptune is concerned. However, all experiments performed so far did not reveal any distinct hint for a ring system. The only confirmed occultation event was that observed on May 24, 1981 (Reitsema et al., 1982). It was interpreted to be caused by a so far unknown third satellite with a diameter of about 100 to 180 km orbiting at a distance of about 3 Neptune radii.

In July 1984 we performed different observing programs using the ESO 0.5 m (R.H.) and 1 m telescopes (J.M.) of the European Southern Observatory. Some days prior to July 22 Drs. Brahic and Sicardy from Paris Observatory called our attention to a star occultation by Neptune expected for that night and provided updated coordinates. Despite the fact that last-minute predictions showed that the planet would very probably miss the star and nothing extraordinary would happen, we decided to "waste" a few hours of our observing time to follow the spectacle.

The technical preparations were done by P. Bouchet and F. Gutierrez, who later on installed the data-acquisition systems at both telescopes. These systems allow integrations in the ms domain and a recording on magtapes. The time is synchronized with the central clock on La Silla every 1 ms. Strip chart recorders were additionally installed to provide on-line information. Since contrarily to the 1 m telescope the 0.5 m telescope has no off-set-guiding system available, continuous measurements have to be interrupted from time to time to check the position of the object within the diaphragm. Therefore, the time needed for a star to cross the diaphragm was determined for different positions along the Neptune track to loose later on as little observing time as possible. Since the star in question, SAO 186001 is very red, we intended to measure in the infrared region in order to enhance the contrast

On the 3 of October while surveying the planet with my twenty-foot Equatoreal having an aperture of 24 inches and with a power applied magnifying 316 times, I was struck with its shape, which was evidently not merely that of a round ball, and again on the 10th. Oct. after applying various powers up to 567 I received many distinct impressions that the planet was surrounded by an obliquely situated ring, thus

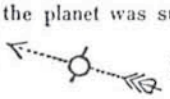

having its major axis nearly at right angles to a parallel of declination, or in other words to the course of the planet through the field.

Fig. 1: *Drawing of Neptune's "ring" as published by W. Lassell in* Astronomische Nachrichten **25,** *357, 1847.*

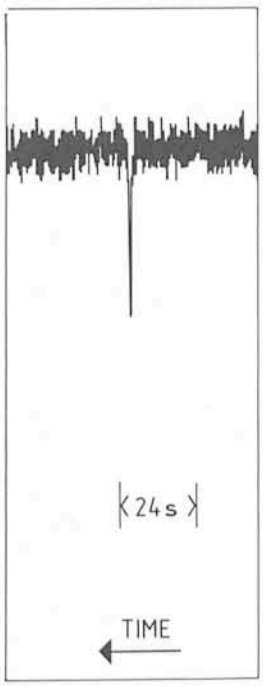

Fig. 2: *Original strip chart recording of the occultation event obtained at the 0.5 m telescope.*

between star and Neptune. We used an I-filter combined with a Quantacon (effective wavelength 0.8 μm) at the 0.5 m telescope and a K-filter (2.2 μm) at the 1 m telescope, which was equipped with the standard infrared photometer. R. Vega was assisting at the 1 m telescope. The on-line magnitudes as determined shortly before the start of the high speed measurements were for Neptune: V = 7.9, I = 9.0 and for SAO 186001: V = 9.2, I = 6.6 and K = 4.2.

The night of July 22, 1984 was of perfect quality: moonless, no cirrus, no wind, seeing around 1″, 10% relative humidity and constant temperature at about 14°C all the time. This was probably due to the fact that a blizzard rushed over La Silla one week earlier and cleared up the skies.

The actual observations (10 ms integration time) were started at the 1 m telescope at about UT 1^h23^m using a diaphragm of 15″. Contrarily to the K-band there was a small contribution by Neptune in the I-band. Therefore at the 0.5 m telescope a diaphragm of 30″ was used and the measurements were started at UT 2^h50^m, when the separation between the star and Neptune was about 15″. This allowed to record the combined flux all the time. The occultation or the closest

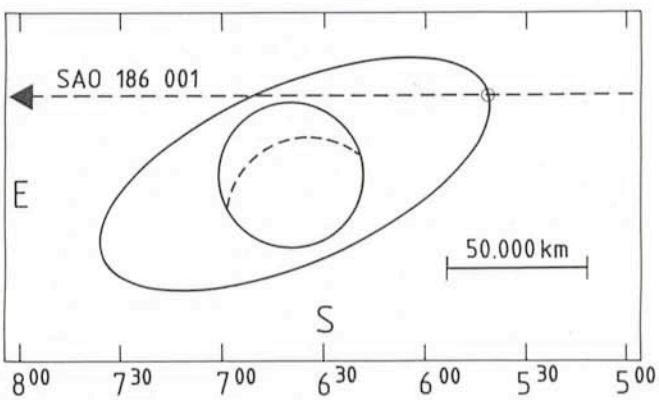

Fig. 3: *Apparent track of SAO 186001. The circle marks the location of the occultation event.*

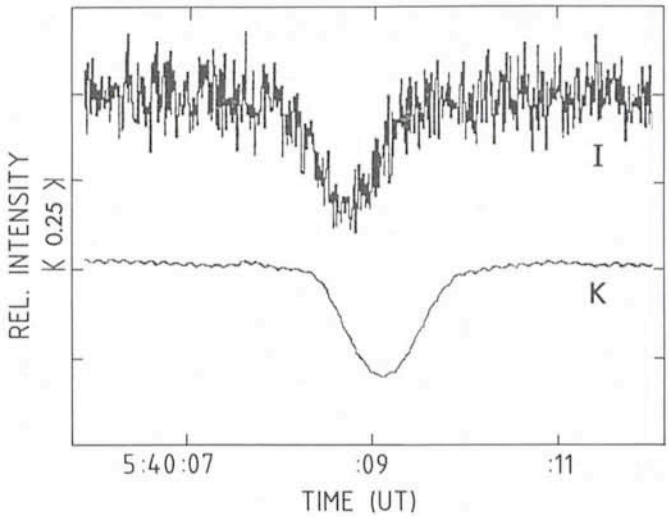

Fig. 4: *The occultation event as recorded by the two telescopes with high time resolution. Time delay and smoothed, wavy shape of the lower curve are due to technical reasons.*

approach was scheduled for about UT 6^h30^m to 7^h. Suddenly, at UT $5^h40^m09^s$ the smooth tracings on our strip chart recorders were interrupted by a very short dip with a duration of about 1.2 s and a depth of about 35% (see fig. 2). Was this the ring so long searched for and did we record it by chance? Thereafter we followed still more intently the things going on. However, nothing particular happened any more; neither an occultation by Neptune nor a second occultation event like the one recorded before was noticed. We continued the measurements till UT 8^h when the very large air mass prevented any further high quality observation. Figure 3 shows the geometry of the appulse as projected on the sky. We telexed the recording of the single occultation event to the IAU Central Bureau for Astronomical Telegrams (Gutierrez et al., 1984) and started immediately with the reduction of the event and with additional measurements.

The differences in shape and timing of the occultation event as recorded by both telescopes (see fig. 4) can be explained in several ways. The telescopes are separated by about 200 m (see fig. 5) so that they were swept by different parts of the shadow of the occulting body. Different diffraction effects could be observed at different wavelengths; the optical

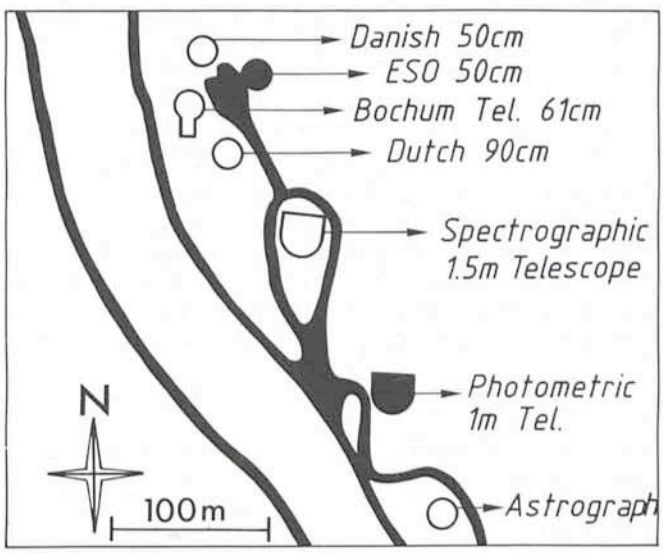

Fig. 5: *Location of the telescopes used on La Silla.*

characteristics of the absorbing material may be wavelength dependent as well as the relative intensities of the involved bodies. Furthermore, the chopping frequencies and the time constants of the infrared equipment induce differences of technical origin.

Previous experience and additional tests showed that the difference in shape as well as the time delay of 0.4 s is about what is to be expected for the 1 m recording because of technical reasons. This means that both telescopes recorded the event simultaneously within an unavoidable error of the order of 0.1 s imposed by the chopping procedure. This, the smooth regular profiles and the clear sky are enough to rule out an occultation by a body close to the Earth (e.g. Earth satellite, cloud, contrails).

A look at the ephemeris of minor planets showed that no catalogued one was in that area. We blinked Schmidt plates taken by H.E. Schuster and O. Pizarro in the following nights 48 hours apart and could not find any unknown moving object down to the 17th magnitude. Closer inspection of the field for fainter, slow moving bodies did not show any object down to the 19th magnitude. Moreover, the probability of such an occultation by a body neither associated with the Earth nor with Neptune, i.e. an asteroid, is extremely low. The coincidence with the Neptune appulse makes the case for the latter association overwhelming, excluding, however, the influence of Neptune's known satellites Triton and Nereid, which were at that time not close to the line of sight.

The orbit of the third satellite proposed by Reitsema et al. (1982) appears to be remarkably similar to that of our object if we assume them to be in the equatorial plane. It is not possible to give a more accurate distance because there was no occultation by the planet itself. The duration of the event combined with the supposed sky-plane velocity of Neptune of about 20 km/s and the shape of the light curve show that we recorded a much smaller body having a chord length of the order of 10 km. On the other hand, the probability of detecting a satellite in that manner is not large and it is nearly impossible to record that new satellite twice. Therefore, in order to enhance the probability we were led to imagine a full ring of bodies of various shapes and sizes circling the planet at a distance of about 3 Neptune radii. This would explain why occultations are not always detected when the orbit passes in front of a star. In particular, we did not detect the second crossing of the orbit which occurred about 1 hour after the first one. However, the irregular nature of this ring does not necessarily imply large, satellite-sized bodies. A ring composed of smaller particles showing an irregular width and optical depth can fit the observations as well. In fact similar rings are known in the Uranus system and perhaps also in the Saturn system. A summary of all these considerations was again sent to the IAU Central Bureau for Astronomical Telegrams at the end of July (Haefner and Manfroid, 1984).

These observational facts imply some theoretical problems: Assuming equal densities for planet and ring material, this ring is located beyond the Roche lobe which conventionally is thought to constitute the outer limit for the existence of such structures. Besides this, the retrograde motion of Triton is sometimes argued to have such an influence that no ring at all can exist. On the other hand the classical resonance theory combined with empirical arguments predicts a possible formation of a ring, although closer to the planet than what we observed (Rawal, 1981). It would then have been formed by tidal disruption of a satellite. This simple resonance law is grossly obeyed within the solar system but there are many exceptions, e.g. as has been shown by the Voyager spacecraft for the fine structure of the Saturnian rings. In fact no satisfactory theory has been worked out so far to explain all ring phenomena in detail.

Five months after our observations we received notice that a nearly identical occultation event had been recorded at the same time by a group of American astronomers working at the Cerro Tololo observatory situated about 100 km south of La Silla (Hubbard, 1984). According to a communiqué from the University of Arizona they "were unable to see the brief event on the computer print-out their telescope generated for every 3.4 s of data". Unaware of our IAU Circulars they did not check their high-speed photometric data (fortunately stored on magtape) before December 1984. These additional observations strongly favour the existence of at least part of a ring having a width of roughly 10–15 km over a length of at least 100 km. This is an unexpected and nice confirmation of our conclusions.

Hopefully more details of the nature of this fragmented ring will be obtained after the launch of the Hubble Space Telescope and during the Voyager 2 rendezvous with the Neptune system in 1989. Probably this spacecraft will need reprogramming to avoid the ring zone on its way to Triton, Neptune's extraordinary satellite.

Acknowledgement

We are very grateful to Drs. Brahic and Sicardy for drawing our attention to this appulse, H.E. Schuster and O. Pizarro for taking the Schmidt plates and to F. Gutierrez and R. Vega for their technical support.

References

Gutierrez, F., Haefner, R., Manfroid, J., Vega, R.: 1984, IAU Circular No. 3962.
Haefner, R., Manfroid, J.: 1984, IAU Circular No. 3968.
Hubbard, W.B.: 1984, IAU Circular No. 4022.
Rawal, J.J.: 1981, The Moon and the Planets **24,** 407.
Reitsema, H.J., Hubbard, W.B., Lebofsky, L.A., Tholen, D.J.: 1982, Science **215,** 289.
Schmeidler, F.: 1985, private communication.

STAFF MOVEMENTS

Arrivals

Europe

BORTOLETTO, Favio (I), Fellow (Astronomical Detectors)
QUATTRI, Marco (I), Mechanical Engineer
SANDERS, Robert (USA), Associate

Chile

GELLY, Bernard (F), Coopérant
HEYDARI-MALAYERI, Mohammad (F), Astronomer
KOEHLER, Bertrand (F), Coopérant
REIPURTH, Bo (DK), Associate

Departures

Europe

BRINKS, Gloria (F), Receptionist
LUND, Glenn (NZL), Engineer/Physicist
MAZZARIOL, Severino (I), Electronics Technician
UNDEN, Christiane (B), Secretary

A Second GEC CCD With UV Sensitive Coating Tested on the CASPEC Spectrograph

The ESO *Messenger* No. 41 contained a short summary of the properties of the CCDs in operation at the La Silla telescopes, among them a GEC CCD (ESO # 6) coated in the ESO lab to enhance the UV-blue sensitivity. A detailed description of the coating technique, the spectral response curve and the first spectroscopic results have been given elsewhere (1). A second GEC CCD was coated and tested successfully in August of this year in the ESO detector lab by Sebastian Deiries and Roland Reiß and it is now available at the telescopes. Its properties are given below.

ESO CCD #7

Telescope:	3.6 m/2.2 m
Chip type:	GEC P8603/A Fluor. coated
Pixel number:	385 × 576, 22 μm in size
e^-/ADU and gain:	6 at G100
Read out noise:	15 e^-
Dark current:	22 ADU/hr at 130°K
Peak quantum efficiency:	55% at 650 nm
Average QE 300–400 nm:	23%

The first spectroscopic tests at the telescope indicate good charge transfer properties. The sensitivity is uniform, with only a few low sensitivity spots and pixels. The quantum efficiency curve is published in (1).

The chip was tested on the ESO echelle spectrograph, CASPEC, with the 52 lines/mm echelle and the short camera.

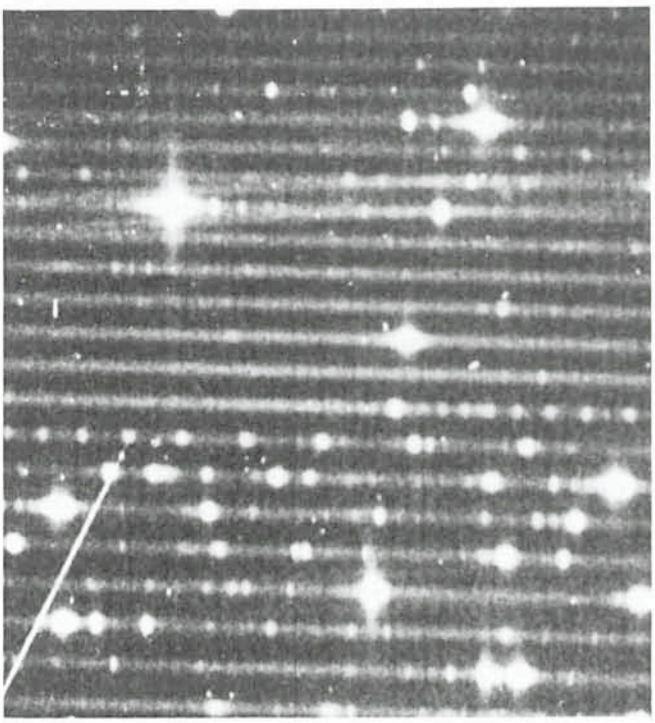

A CASPEC spectrum of the slow nova RR Tel centered on 350 nm and covering about 100 nm. A GEC CCD coated in the ESO lab to enhance the UV sensitivity was used as a detector (ESO CCD #7). The resolving power is 22,000, the exposure time 30 m. The bright streak in the upper-left corner is present in this frame only and it is probably due to an energetic cosmic ray.

With this combination, the orders are well separated down to 310 nm and full spectral coverage is obtained to about 420 nm. The figure shows the UV spectrum of the slow nova RR Tel at a resolving power of about 22,000. From an observation of the standard star LTT 7987 (2) with a wide slit, the efficiency of the atmosphere-telescope-spectrograph-detector combination at 350 nm is such that 1 photon/A,s is recorded at 350 nm from a star of $m_{350} = 14.3$, where the magnitude is related to the flux in ergs s^{-1} cm^{-2} Hz^{-1} by the expression $m = -2.5 \log f_\nu - 48.6$. *S. D'ODORICO*

References

(1) Cullum, M., Deiries, S., D'Odorico, S., Reiß, R., 1985, *A & A*, in press.
(2) Stone, R.P.S., Baldwin, J.A., 1983, *M.N.R.A.S.* **204,** 347.

MIDAS Memo

ESO, Image Processing Group

This is the first appearance of the "MIDAS Memo" which is intended to be a regular contribution to the *Messenger* with the purpose of informing the ESO community at large of the developments, plans, and changes in the Image Processing Group in Garching. It will deal primarily with subjects related to data analysis and the MIDAS image processing system, but will also report from time to time on other aspects of the Image Processing Group's activities such as the measuring machines, the developments in archiving of data from La Silla, computer operations and policies, as well as activities related to computer to computer communications.

1. Application Developments

This will be a regular subsection of the "Memo", but will only be able to highlight recent developments and future planning and not report in detail on all the minor enhancements and changes to the MIDAS system in the intervening period.

The MIDAS table file system continues to grow as a tool for a wide range of applications. In connection with the ST-ECF project to build models of the various ST instruments, several new facilities have been added as general purpose table system functions. These include: In part new commands, access to tables from any disk directory, and more detailed explanation of errors.

The suite of programs for reducing CASPEC data has been widely used in the last year, and has recently been greatly enhanced to permit many automatic procedures. Work on the determination of absolute fluxes is in progress.

A generalized suite of programs for spectral analysis is in the process of being developed and documented. Although not specifically optimized for any particular instrument or type of data, advanced capabilities to extract and manipulate two dimensional spectra will definitely be a part of this development. In addition, these facilities will handle CES data, EFOSC spectral data, Optopus data and so on.

2. Device Independent Graphics in MIDAS

After a long search for a simple yet effective device independent graphics system, the Astronet Graphics Library has been chosen to be implemented into the MIDAS system. This library has its origins within the Astronet project in Italy and met most of the criteria for the functionality of such a product. In particular, it is not proprietary as many commercial packages such as GKS are and does not require a license if used by academic or research organizations. The AGL library has the necessary subset of the GKS functionality for the MIDAS applications and is an efficient implementation of this functionality. Also it is supported by a strong group within the Astronet project that will insure its continued viability and adaptability in the future. It is anticipated that a release of the MIDAS system in the spring of 1986 will be adapted to the AGL library and will provide drivers for many of the standard graphics devices. In particular, better support of the almost Tektronix compatible family of graphics terminals is anticipated. A definitive list will be provided in a future "MIDAS Memo".

3. Device Independent Image Display Software

After the ST-ECF meeting in Paris in May, it became quite evident that there is a strong desire on the part of many users that some sort of device independent interfaces for image displays be developed along the lines of the device independent graphics standards. These interfaces would allow various image displays to be used with the MIDAS software or with any software that implements these interfaces. This is a more difficult problem than the graphics question since there are as yet no standards such as GKS available to serve as a model. Progress is nevertheless being made. A preliminary draft has been drawn up in collaboration with the STARLINK project in the UK and it is hoped that this set of interfaces will be mature enough for discussion by a wider audience in early 1986. Of course, the time scale for implementing these interfaces into MIDAS and providing support for various other display devices besides RAMTEK and DeAnza is still to be defined. Suggestions are more than welcome at this time and should be directed to Klaus Banse.

4. ESO Archives

The development of archiving of ESO data is proceeding in parallel with the Developments for the Space Telescope "Data Management Facility", and will share in principle the same hardware and most of the same software so that an integrated archiving system will exist.

On the hardware side, ESO is sharing 50 % of a data base computer known as "Intelligent Database Machine". This device implements hardware that permits fast searching of relations between various data. Also, an optical disk has been acquired for the permanent storage of data. Both these devices are in the process of being installed and tested in Garching and are not yet available for public access.

On the software side, programs and procedures are being developed in close collaboration with the ST-ECF and the Space Telescope Science Institute. This software will provide the necessary tools to determine what observations have been made and to retrieve data from the permanent storage. More on these developments will be available in future columns.

Spectrophotometry of Globular Cluster Stars with the CASPEC System; A Comparison with Results from Other Spectrographs

F. SPITE, P. FRANÇOIS, M. SPITE, Observatoire de Paris-Meudon

I. What is the Aim of Abundance Determination in Globular Cluster Stars?

The globular cluster stars, as well as the field halo stars, are among the oldest observable objects of our Galaxy and even of the Universe. The abundance of metals in their atmosphere is small; it is the signature of still older objects which synthesized these metals out of the primordial material (essentially made of hydrogen and helium). The analysis of globular cluster stars provides a unique opportunity to understand the early history of our Galaxy.

During the last ten years, as échelle spectrographs were available at the Kitt Peak and Cerro Tololo 4 m telescopes, numerous globular cluster stars were analysed in detail (see for example the review paper of Pilachowski et al. 1983). Interesting information was gathered but a number of problems appeared.

In particular, it seems that although field halo stars and globular clusters were formed simultaneously (Carney 1979) there are some differences in the chemical composition of globular cluster stars and of the field halo stars. For example, it has been noted that in globular cluster stars the strength of the CN and the CH bands varies from star to star and in some clusters sodium and aluminium appear enhanced in "CN strong" stars.

It has been suggested (Iben and Renzini, 1984) that this phenomenon could be due to the crowding of the stars in a cluster: this crowding would lead to an accretion of the ejecta of intermediate AGB stars onto main sequence dwarfs (at the beginning of the evolution of the globular cluster). These ejecta

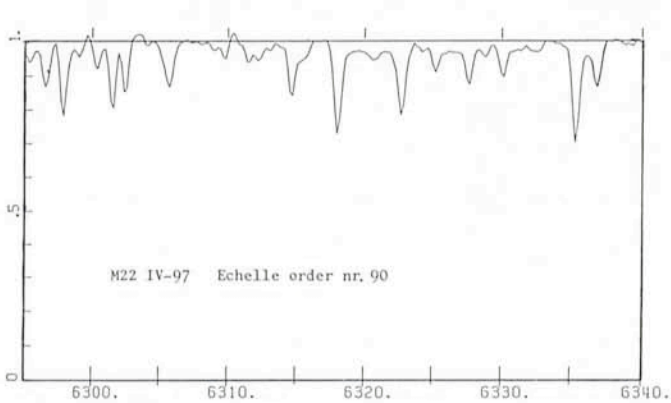

Fig. 1: *An example of a part of an echelle order.*

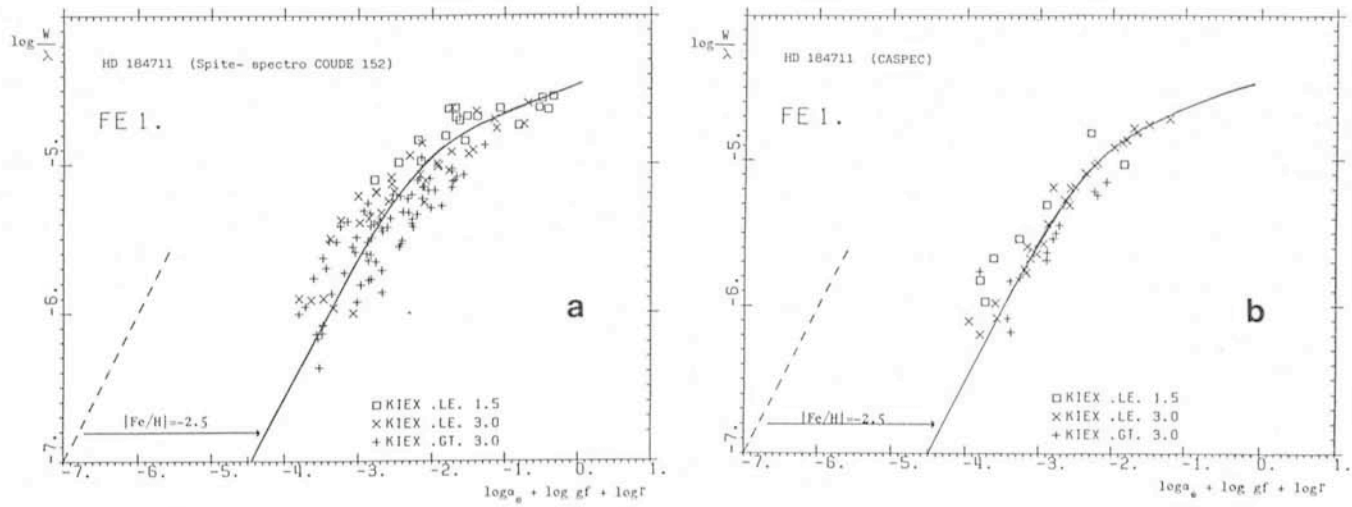

Fig. 2: *Curves of growth of HD 184711: (a) from photographic spectra (1.52 m telescope, coudé spectrograph); (b) from CASPEC spectra.*

could be enriched in carbon, nitrogen, sodium and aluminium according to Iben (1975).

A good way to test this explanation is to compare with high precision the relative abundances of the elements in the atmospheres of the globular cluster stars and of the halo field stars.

It is clear that the abundance anomalies that are expected in globular cluster stars are rather small (a factor of 2 or 3) and, therefore, their measurement requires a high accuracy in the determination of the abundances, especially when the element is represented by only a few lines and when these lines are weak.

II. The CASPEC Spectrograph and the Precision of the Data

First, we wondered whether the resolution of the CASPEC spectrograph was sufficient to study the abundance anomalies in globular cluster stars.

A first run of three nights was allocated at the 3.6 m telescope in June 1984. The weather is not always good in June but in spite of high winds, clouds and bad seeing we could obtain at least the spectra of one supergiant star in M22 and of one in ω Cen, as well as the spectrum of a typical halo field giant, HD 184711, as a reference star.

The 31.6 l/mm echelle and the 300 l/mm cross disperser gratings were used, which give a dispersion of 6 Å/mm and a resolution of 20,000. The ADU of the star spectra was about 1,000. Flat-field exposures were taken after each object exposure, using the quartz lamp. The reduction of the data was partly carried out at the ESO Garching facilities where the help of D. Ponz was greatly appreciated, and partly with our own programs on the VAX computer at Meudon; we checked that both reduction packages give the same results. An example of the tracing of the spectra is given in figure 1.

III. Comparison with a Star Previously Observed with Another Spectrograph: HD 184711

We first compared the results of the CASPEC with those of the 1.5 m coudé spectrograph. Some years ago, indeed, we obtained spectra of the field halo giant HD 184711 with this spectrograph (Spite and Spite 1979). The resolution of these spectra was approximately the same as the one of the CASPEC spectra but the range of wavelength was different (λ4300–6200 for the coudé spectra and λ6000–6900 for the CASPEC spectra). Thus the easiest way to compare the precision of the abundance determination was to compare the observed curves of growth built from the same model atmosphere with both sets of data. These curves of growth are

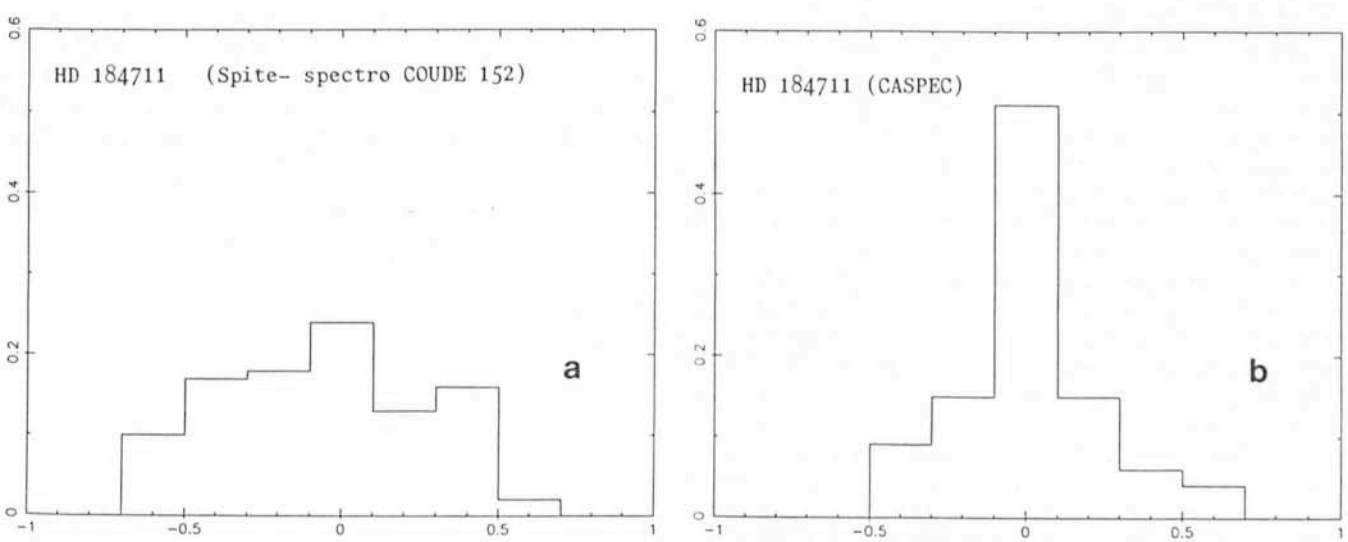

Fig. 3: *Histogram of the dispersion of FeI measurements around the curve of growth: (a) from photographic spectra (1.52 m telescope coudé spectrograph); (b) from CASPEC spectra.*

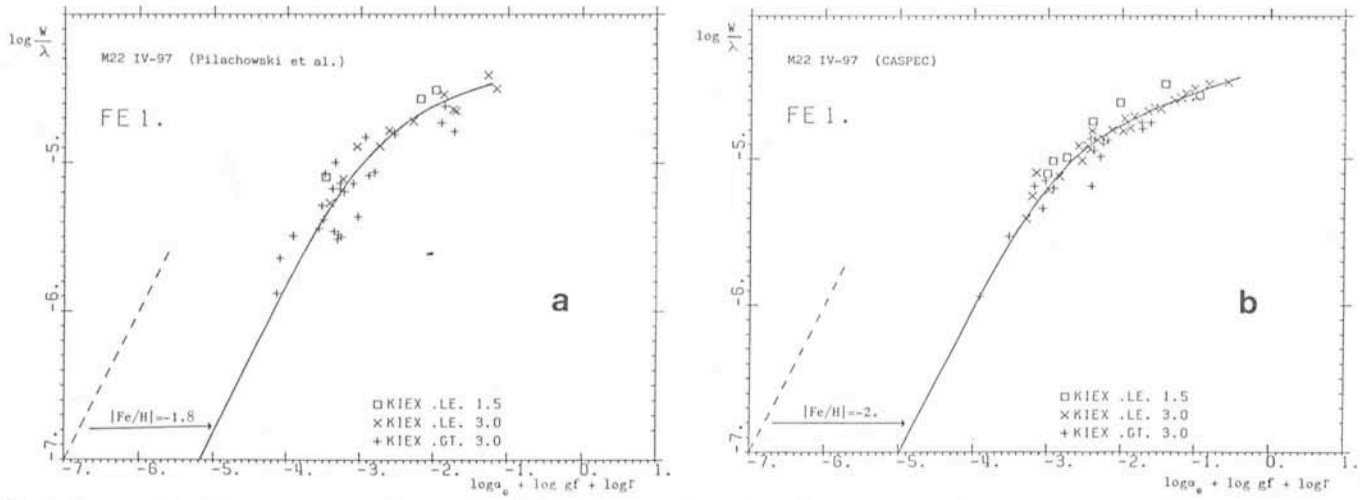

Fig. 4: *Curves of growth of M22 IV97 from echelle spectra: (a) at Kitt Peak (Pilachowski et al. 1982); (b) at ESO (CASPEC).*

displayed in figures 2a and 2b. The ordinate is log W/λ where W is the equivalent width of the line, and the abscissa is X = $\log\alpha_O$ + log gf + logΓ where α_O is the abundance of the element in the solar atmosphere, gf the oscillator strength of the line and Γ a parameter depending on the model and on the line (Cayrel and Jugaku 1963) computed line by line from the model of the star. The abundance of an element relative to the Sun ([Fe/H] for example) is then simply represented by the distance between the linear part of the curve of growth and the fiducial line logW/λ = X (fig. 2).

It can be seen, at first, that the mean abundance [Fe/H] = −2.5 is the same in figures 2a and 2b. But the standard deviation is smaller when the CASPEC data are used. This is striking in figure 3 where the histograms of the deviations of the abundances measured line by line, from the 1.5 m coudé photographic spectra and from the CASPEC spectra, are compared.

IV. Observation of a Star Already Observed at Kitt Peak: M22–IV97

This star is one of the brightest in M22. It has already been analysed by Pilachowski et al. (1982) using 6 Å/mm KPNO spectra in the range λ5300–6300 Å. We obtained a spectrum of this star in the range λ6000–6900 Å. The theoretical and observed curves of growth for the KPNO and the CASPEC data are drawn in figures 3a and 3b, and the histograms of the abundances computed line by line in figures 4a and 4b. Again the quality of the CASPEC data seems excellent.

Moreover, part of the abundance spread along the curve of growth is probably real. It can be seen indeed, in figure 3b, that the Fe abundance deduced from the low excitation potential lines (open squares) is higher than the abundance deduced from the high excitation potential lines (crosses). This phenomenon points towards a possible error on the temperature of the model or more probably a non-LTE effect in the atmosphere, leading to an over-population of the lower levels of the atom. To avoid this effect as far as possible, it is generally recommended not to use the low excitation potential lines in an abundance determination.

V. The Chemical Composition of M22–IV97 and ω Cen 65

Therefore, although the CASPEC echelle spectrograph arrived late at ESO we are convinced that many interesting works can be done with this excellent instrument, in particular about the chemical composition of the old galactic objects like the globular cluster stars (see also D'Odorico et al. 1985).

In Table 1 we present our preliminary abundance determinations in the atmospheres of the stars M22–IV97 and ω Cen 65.

The atmospheres of the stars have been simulated by models interpolated in the grid of the Gustafsson's models (Gustafsson et al. 1975) extended toward lower gravities and temperatures (Gustafsson 1977). Line transition probabilities were determined from a line by line analysis of the solar spectrum (Delbouille et al. 1973). For this work the Holweger solar model has been used (Holweger, Müller 1974). The damping constants of the lines were taken by adding 0.78 dex to the Van der Waals constant computed from the hydrogenic approximation of Unsöld (Aller, 1963).

The two stars are rather similar (the mean abundance of the elements is about 1/100 of solar abundance). Differences appear for Na, Al and Ba. Some recent theories can account for such anomalies.

The gravities of the stars have been computed by admitting that the star masses were about 0.8 $M_\odot$. It is clear that in this case the ionization equilibrium cannot be satisfied: the iron abundance is different when the neutral or the ionized lines are used. On the other hand, we are also able to confirm an H_α

TABLE 1
Abundance of the elements relative to the Sun

	M22 IV–97	ω Cen 65
Stellar parameters: θ_{eff}, log g, [M/H] v_t	1.26, 0.9, −1.9 2 km/s	1.26, 0.3, −1.8 2 km/s
Element	log ($A_\star/A_\odot$)	log ($A_\star/A_\odot$)
O I	−1.9	−1.8
Na I	−1.9	−2.3
Al I	−1.5	−1.1
Si I	–	−1.2
Ca I	−1.6	−1.5
Sc II	−1.7	−1.9
V I	−1.9	−1.9
Ti I	−1.6	−1.7
Ti II	−1.4	−1.4
Cr I	−2.3	−2.1
Fe I	−2.0	−1.9
Fe II	−1.4	−1.5
Ni I	−1.9	−1.9
Ba II	−1.3	−1.9

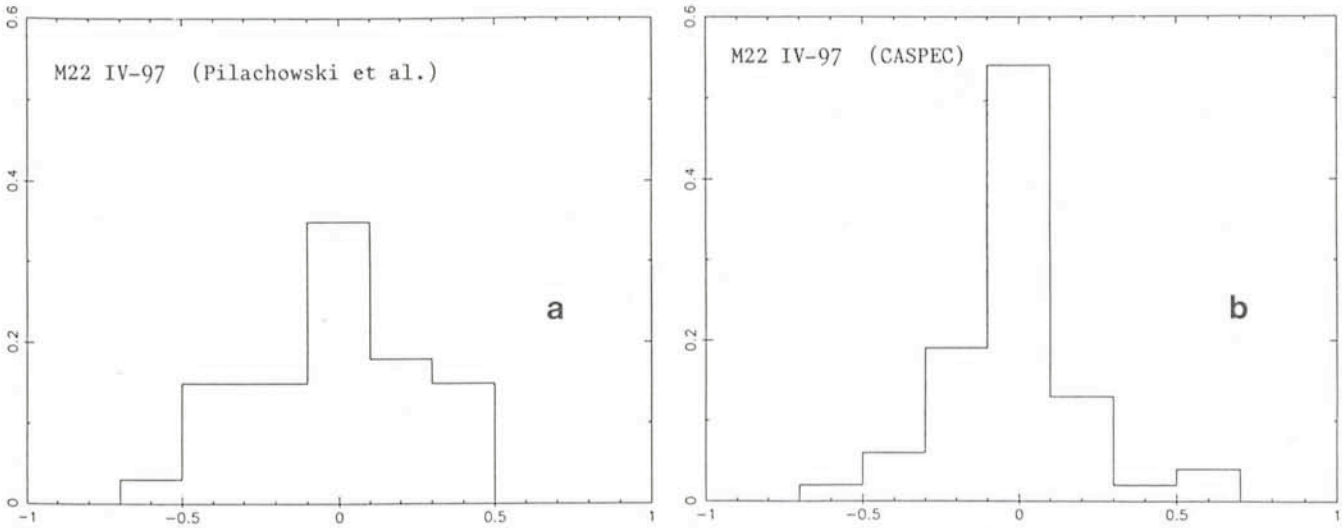

Fig. 5: *Histogram of the dispersion of Fe I measurements of the star M22 IV97: (a) at Kitt Peak (Pilachowski et al. 1982); (b) at ESO (CASPEC).*

emission in these globular cluster stars and in the active star HD 184711 (Spite et al. 1981; Gratton et al. 1984).

In addition, we recently obtained some other excellent spectra of stars in ω Cen, NGC 6582, and in the Magellanic Clouds (field stars and globular cluster stars). All these spectra are now under reduction and seem very promising.

We are very grateful to Dr. D'Odorico for advising us about the optimal use of CASPEC and CCD for our program.

References

Aller, L.H.: 1963, *The Atmosphere of the Sun and Stars,* 2nd edition, Ronald Press, New York, p. 320.
Carney, B.W.: 1979, *Astrophys. J.,* **233,** 877.
Cayrel, R., Jugaku, J.: 1963, *Ann. Astrophys.* **26,** 495.
Delbouille, L., Roland, G., Neven, L.: 1973, *Photometric Atlas of the Solar Spectrum from λ 3000 to 10000 Å,* Liège: Institut d'Astrophysique de Liège (presently available from λ3600 to 8000 Å).
D'Odorico, S., Gratton, R.G., Ponz, D.: 1985, *Astron. Astrophys.,* **142,** 232.
Gratton, R.G., Pilachowski, C.A., and Sneden, C.: 1984, *Astron. Astrophys.* **132,** 11.
Gustafsson, B., Bell, R.A., Eriksson, K., Nordlund, A.: 1975, *Astron. Astrophys.,* **42,** 407.
Gustafsson, B .: 1977 (private communication).
Holweger, H., Müller, E.A.: 1974, *Solar Phys.,* **39,** 19.
Iben, I.Jr.: 1975, *Astrophys. J.,* **196,** 525.
Iben, I.Jr., Renzini, A.: 1984, *Physics Reports,* **105,** no. 6.
Pilachowski, C., Sneden, C., Wallerstein, G.: 1983, *Astrophys. J. Suppl.* **52,** 241.
Pilachowski, C., Wallerstein, G., Leep, E.M., Peterson, R.C.: 1982, *Astrophys. J.,* **263,** 187.
Spite, M., Caloi, V., Spite, F.: 1981, *Astron. Astrophys.,* **103,** L11.
Spite, M., Spite, F.: 1979, *Astron. Astrophys.,* **76,** 150.

High Resolution Monitoring of the Emission Lines in SS 433

P. ANGEBAULT[1], S. D'ODORICO[1] and G. MILEY[2]

[1] *European Southern Observatory*
[2] *Space Telescope Science Institute, Baltimore, and affiliated to the Astrophysics Division, Space Science Dept. of the European Space Agency, Noordwijk. On leave from Leiden Observatory.*

Introduction to SS 433

During the last few years the star 433 of the Stephenson Sanduleak catalogue of emission-line objects has become one of the most intensively observed sources in the Galaxy. It is believed to be an X-ray binary whose compact component is either a neutron star or a black hole. Attention was drawn to SS 433 in 1978 by Clark and Murdin (1978), who pointed out that independently discovered X-ray and radio sources were probably associated with SS 433. The object is situated at the center of a supernova remnant detected at radio wavelength (W 50) and showing Wolf-Rayet like winds.

It was in 1979 through a study of its optical spectrum by Bruce Margon that SS 433 entered the astronomical hall of fame. The spectrum is dominated by Hα emission lines although HeI, HeII and CIII/NIII are also present, as well as stellar and IS absorption lines. The remarkable discovery was that the Hα lines were split in three components. Two of them oscillate with opposite phase over a huge radial velocity range (−30,000 to +50,000 km/s) with a 164-day period. Shortly after Margon's discovery, Andy Fabian and Martin Rees suggested that these moving "satellite" lines arise in two oppositely directed jets and the kinematic "precessing jet" model developed in detail by Abell and Margon has had remarkable success in explaining observations of SS 433. Precession of the (v = 0.26c) jets was invoked to explain the 164-day period (see e.g., Margon, 1984). Beautiful confirmation of this precessing jet model was provided by radio measurements by several groups which showed that SS 433 is resolved on various scales from less than 3 milliarcseconds up to 2 arcseconds, is jet-like and has a changing corkscrew structure which varies in good agreement with predictions of the model

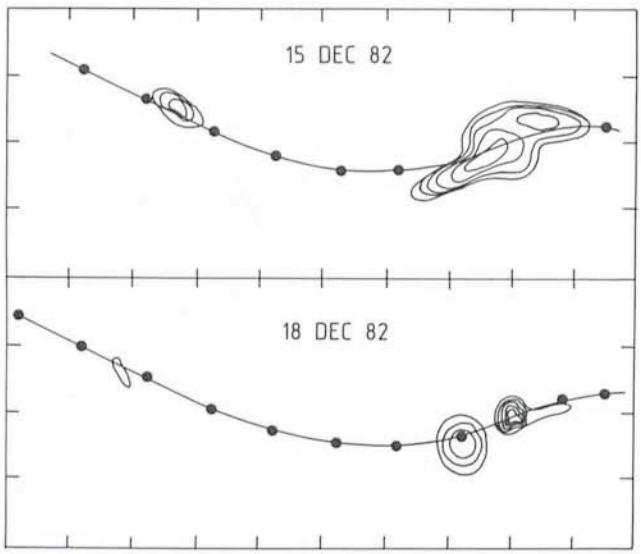

Fig. 1: *Contour maps of SS 433 showing the evolution of the structure in time; the solid lines represent the expected trajectories of blobs on the kinematic model (Schilizzi et al. 1984).*

derived from optical spectroscopy (see fig. 1). The radio measurements provided one more in a chain of tantalyzing similarities between nonthermal radio emission in stars and active galaxies.

Gravitational accretion and radiation pressure are often invoked to explain the acceleration of particles in the stellar jets; the confinement of the beams is believed to result from the presence of a magnetic field or from the rotation of the system. Independently of detailed models, there is considerable evidence that SS 433 is an X-ray binary whose compact component is either a neutron star or a black hole. The optical radiation obviously originates both from a central source (accretion disk and illuminated companion), and also from rapidly moving regions which are in interaction with the ISM and responsible for the Doppler-shifted recombination lines; the companion star is likely to be dominated by the accretion disk.

The Purpose of the High Spectral Resolution

One of the most intriguing questions regarding SS 433 concerns the exact relationship between the relativistic plasma responsible for the synchrotron radio emission and the ionized gas which emits the optical lines. In the case of extragalactic jets, several cases of morphological associations have been found between radio-continuum and optical-line knots implying that as a jet propagates through the ambient medium it can interact vigorously with its environment. Could the satellite emission lines in SS 433 be produced by similar processes?

In an effort to relate the changing details in the Hα profile to the moving blobs in the radio jet, we have used the CASPEC echelle spectrograph on the 3.6 m telescope to monitor the spectrum of SS 433 simultaneously with VLBI measurements of the radio structure being carried out by a group which includes Richard Schilizzi (Dwingeloo), Renee Vermeulen and Vincent Icke (Leiden), Richard Spencer (Jodrell Bank), Richard Porcas and Istvan Fejes (Bonn) and John Romney (NRAO). During this campaign which lasted two weeks, Paul Murdin also obtained a set of medium resolution optical spectra using the 2.5 m Newton telescope at La Palma, and X-ray observations with the Exosat satellite were obtained.

Until now little data were available on the emission line profiles of SS 433 with resolutions of better than a few

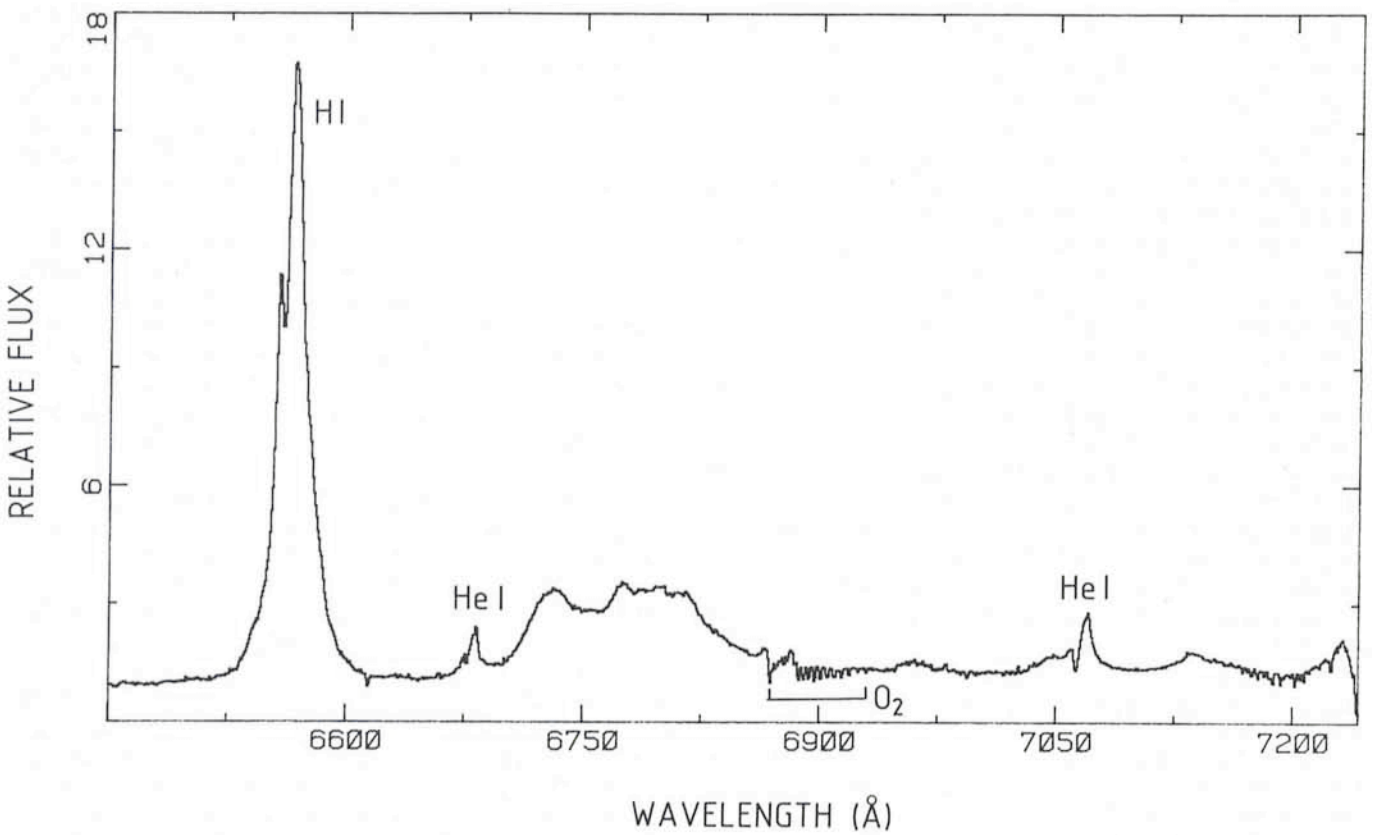

Fig. 2: *SS 433 shows a composite spectrum of steady emission lines and Doppler-shifted lines known as "moving lines". This spectrum has been obtained with CASPEC at the ESO 3.6 m, in a 40 mn exposure. The emissions observed here are HI (6563 Å), HeI (6678 and 7065 Å) and their broad shifted counterparts. In addition, possible P-Cygni profiles are observed in the steady HeI lines.*

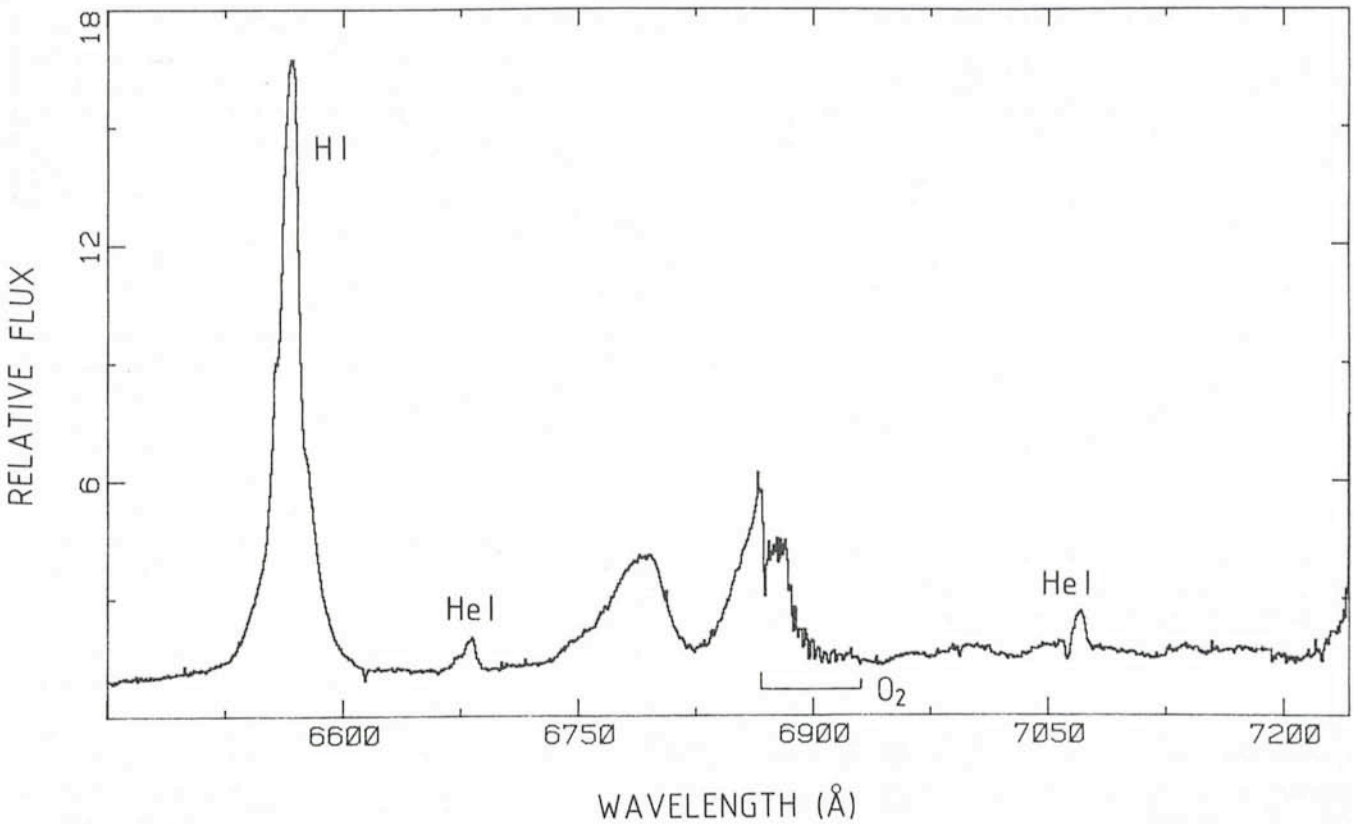

Fig. 3: *An example of unexpected emission regarding the precession period; the two features at 6790 and 6860 Å cannot easily be explained by the standard kinematic model.*

angstrom. It was our hope that observations of the lines at high spectral resolution coupled with the radio maps would give a unique tool for probing possible interactions.

Several further observational facts about SS 433 remain difficult to explain using the standard model, among them sudden fluctuations and disappearances of the moving lines, the great number of harmonics of the precession period and the energy necessary to power the beams. With the hope of investigating some of these questions we decided to carry out high spectral resolution monitoring of SS 433.

Thanks to the high through-put of the telescope/spectrograph/detector combination (around 6 percent efficiency), we were able to obtain, using integration of the order of 40 minutes, high S/N spectra of SS 433 over a range of 1000 Å, with a resolution of 0.65 Å.

We used CASPEC together with the 31.6 l/mm grating. Since SS 433 is faint (magnitude 14.2 .5 in V), we applied electronic binning of the CCD in order to reduce the effect of the read-out noise. Eleven spectra were obtained between May 19 and June 3. They have been reduced with the echelle reduction package in the MIDAS data analysing system running on the VAX 780 at ESO-Garching. The accuracy of the wavelength calibration was found to be better than .07 Å, when checked on the He-Ar lines of the comparison lamp spectrum.

Preliminary Results from the CASPEC Data

Figures 2 and 3 show two of the reduced spectra. The data have still to be fully analysed, but some preliminary findings are summarized below.

On the basis of the precession period, we expected to find three Hα components; a zero velocity one (in fact red-shifted by 100 to 300 km/s depending on the phase of the orbit), a red component varying between 6950 Å and 6700 Å and a blue component varying between 6600 Å and 6900 Å.

(i) It is clear that the moving lines are generally resolved and that they show complex structures which one might interpret as a result of a clumpiness of the beams, implying that different velocity clouds show up simultaneously in the line of sight. As a consequence of observations made on one night where two spectra were obtained with a time separation of only 2 hours, we were able to observe that these structures evolve extremely rapidly.

(ii) The zero velocity Hα component shows a complex and variable profile. In particular, a feature is observed on the blue wing and its variations seem to be related neither to the precession period, nor to the orbital one; this would support the interpretation that the double Hα profile is a variable self-absorption although a more complete investigation will be necessary to reject the hypothesis of a blue-shifted emission. Moreover, variable P-Cygni profiles seem to be present in the He I steady emission lines.

(iii) In addition to the predicted Hα satellite lines, strong unidentified emission lines are seen in two of our spectra, fading out in less than three days (cf. fig. 3).

(iv) To explain the position of the satellite lines within the framework of the standard kinematic model we needed to apply a phase shift of about .02 (3 days) to our observations. Although this shift is contained within the observed scatter of the fitted precession period, the complexity of the spectra makes it very difficult to find a symmetric evolution of the line around 11,000 km/s, as suggested by the kinematic model, and our data are therefore not sufficient to properly constrain the ephemeris (cf. fig. 2). If we accept this phase shift as being real, we can explain the deviation from the model by keeping in mind the great number of harmonics found in the velocity curve, which produce a scatter of up to 100 Å in the line cen-

ters. This scatter should be correlated between the two shifted lines.

It is clear that, by combining our data with those obtained in La Palma at about the same time, we will be able to reach a more complete understanding of these phenomena.

What Can We Expect from the Comparison of Optical and VLBI Data?

The VLBI observations are at present being reduced and should be available within a few months. Comparison of the two data sets will then be attempted. If moving features in the optical spectrum appear to be correlated with changing blobs in the radio jet, the origin of the Hα emission will be determined; this would provide a new possibility for mapping of the ionized gas structures, since until now imaging in the optical range has not shown any extended features around SS 433. In addition, detailed kinematic mapping of the propagation of the SS 433 jet could be envisaged with the Space Telescope, if the data correlation proves positive.

Particular attention will be paid to the following points:

- Does the bending of the radio jets affect the velocities of the moving lines?
- Is there any relation between the production of blobs and the equivalent width of the zero velocity Hα line?
- How is the spectacular appearance and disappearance of emission lines manifested in the radio data?

There are other X-ray stars which are known or suspected to present similarities with SS 433 and with the grander but more distant phenomena seen in AGNs (e.g., Sco X-1, Cir X-1, Cyg X-3, Her X-1 . . .), but none of them has revealed in such an open manner its intense private life. If SS 433 decided to cooperate with us last summer, important new information about the nature of X-ray binaries and even about jets in AGNs may result. It's now up to SS 433!

References

Abell G.O. and Margon B., *Nature* **279,** 701 (1979).
Clark D.H. and Murdin, P., *Nature* **276,** 44 (1978).
Fabian, A.C. and Rees, M.J., *M.N.R.A.S* **187,** 13 P (1979).
Margon, B., in *An. Rev. of Astr. and Astroph.* **22,** 507 (1984).
Schilizzi, R.T., Romney, J.D. and Spencer, R.E., IAU Symp. **110,** 289 (1984).

T Tauri Stars Through the Looking-Glass

U. FINKENZELLER and G. BASRI, Astronomy Department, University of California, Berkeley

The Red Queen shook her head. "You may call it 'nonsense' if you like," she said, "but I've heard nonsense, compared with which that would be as sensible as a dictionary!"

Preface

The CASPEC on the 3.6 m telescope is a very powerful new instrument for high dispersion spectroscopy. We have used it (in conjunction with an IDS) to obtain almost all the optical information possible on a number of T Tauri stars, namely calibrated resolved full spectral coverage. The analysis of such a large amount of information will take quite some time; the purpose of this contribution is primarily to acquaint other users with some of both the joys and pitfalls of this instrument which we feel are worthwhile to publicize. We also describe a little of the science in our particular project.

Chapter I

"It seems very pretty," she said [. . .], "but it's rather hard to understand!" (You see, she didn't like to confess, even to herself, that she couldn't make it out at all.)

T Tauri stars are young stellar objects with emission line spectra and complex atmospheres. Found in the upper right of the Hertzsprung-Russel diagram, they have effective temperatures from 3,000 to 6,000 K, and are estimated to be between 10^5 and 10^7 years old. Numerous observations in all parts of the electromagnetic spectrum indicate differences in activity levels of up to three orders of magnitude, together with temporal variations ranging from the beginning of astronomical data taking down to a few minutes. Due to their generally complex nature and the difficulties in obtaining a fully useful set of observational material, relatively little attention has been paid so far to self-consistent physical modeling of these stars. We have made an observational effort to provide new material which will allow the use of "classical" diagnostic tools to obtain detailed structures for most of the stellar atmosphere.

Guided by the rule that physical processes are most easily analyzed in their least complex manifestation, we have chosen seven low to intermediately active T Tauri stars (rather than exotic objects) from the spectral catalogue of Appenzeller et al. (1983). For further references on the stars, see also the original list of Schwartz (1977). The target objects span from G2 to M0 in spectral type, and from 5.8 to 0.5 in $L_\odot$ (see table). We have three pairs consisting of objects which are almost identical in most parameters, except for activity level. Together with a carefully chosen set of standard stars we are in a position to perform a differential activity analysis from the main sequence into the pre-main sequence domain by extrapolating proven diagnostic methods to slightly "perturbed" objects.

Chapter II

"I should see [. . .] far better," said Alice to herself, "if I could get to the top of that hill."

The full astrophysical potential for modeling of PMS stellar activity can only be realized if based on resolved flux calibrated, and high S/N spectra obtained for many diagnostics at the same time. With most instruments, the simultaneous demands of extreme spectral resolution and accurate spectrophotometry mutually exclude each other since the slit size affects both quantities in opposite ways. Thus, we used two different spectrographs concurrently: The ESO echelle spectrograph with CCD (CASPEC) at the 3.6 m and the IDS at the 1.5 m telescope. With a slit size of 3″ × 3″ at the former and 8″ × 8″ at the latter instrument we achieved resolutions of about 12,000 and 500–1,000, respectively. (The IDS grating was used in both first and second order.) The spectrophotometric observations had to be done strictly concurrently, since T

T TAURI STARS COVERED FROM 3800 TO 8700 Å

Star	Assoc.	m_v	Sp	$L_\odot$	$W_\lambda(H_\alpha)$	$W_\lambda(H_\beta)$	W_λ(HeI5876)	W_λ(LiI6707)
Sz06	Cham. 1	11.2	K2	2.34	−31.9	−2.30	—	0.43
Sz19	Cham. 1	10.6	G2	5.85	−14.6	−0.13	−0.04	0.23:
Sz65	Lupus 1	12.2	K7-M0	—	−24.2	+0.90	−0.79	0.61
Sz68	Lupus 1	10.5	K2	2.80	− 4.9	+1.95	—	0.42
Sz77	Lupus 1	12.5	M0	0.50	−15.1	−0.91	−0.21	0.60
Sz82	Lupus 2	12.2	M0	0.83	− 4.6	−0.03	−0.19	0.57
Sz98	Lupus 3	12.4	K8	0.72	−17.8	+3.39	−0.16	0.51

Tauri stars are expected to show irregular temporal variations, on top of which a rotational modulation may be imposed.

Apart from avoiding the principal limitations mentioned above, this scheme of observing allowed a most efficient use of the 3.6 m telescope, since no time had to be spent on observing mostly faint flux standards. Even more important, this technique avoids a number of cumbersome calibration problems which would have to be solved if one were to rely fully on CASPEC data alone (see below).

We were guided by the desire to cover the most important lines of CaII and hydrogen along with photospheric lines of all strengths, which demanded contiguous spectral coverage from 3800 Å to 8700 Å. Four echelle frames were required to span this spectral range, with a gap from 6700 Å to 7700 Å. With the 31.6 g/mm grating and the standard cross disperser complete order overlapping resulted, even in the near IR (8 Å at 8700 Å, rising to 36 Å at 3900 Å). A final total of 602 echelle orders of T Tauri stars and 560 orders of spectroscopic standards, supplemented by accompanying IDS scans, were obtained in three nights.

Chapter III

She puzzled over it for some time, but at last a bright thought struck her.

The IDS data were reduced according to standard procedures. The only minor problem arose with Baldwin and Stone's (1984) white dwarf standards which had to be resampled in order to tighten the grid for the response curves at the chosen resolution.

The CASPEC data were initially processed with the packages available in MIDAS for echelle work. However, we soon realized certain limitations which have to be faced when one is doing work in the ultraviolet where the spacing of the orders is steadily decreasing. (And it is in the ultraviolet that more astrophysical interesting lines happen to be than anywhere else.) At this point the reference to the external calibration from the IDS greatly helped in avoiding those internal problems shortward of 5000 Å as described below.

In an echelle frame centered at 4300 Å and taken with the standard cross disperser 33 orders are present, ranging from 3700 Å to 4765 Å. Since the RCA chip used is 321 pixels by 516 pixels, each order is about 9 pixels wide perpendicular to the dispersion, interorder background included. Under these limitations, useful work can only be done with the smallest entrance slit available, i.e. 3″ × 3″. Much thought has gone into the MIDAS echelle software which cannot be explained in detail here. The positions of the orders on the chip are recovered by two finding algorithms: Any specific order is first located once in the column running vertically through the middle of the frame and then defined by a maximun-following algorithm in both directions from this position. Both algorithms use polynomial fits, the recommended default degrees are 1 for the former and 2 for the latter.

Experience has shown, however, that it is hard to accomplish a global good fit for all regions within a frame. Polynomial degrees too low will not take into account small spatial variations or the slight distortions introduced by the spectrograph camera. On the other hand, polynomial degrees too high will introduce the well known wiggling effects which make the software slit run across the signal like a drunken driver speeding on a highway. Both effects are worst at the extreme ends of *all* orders in general, and the *uppermost* and *lowermost* orders of a particular frame. In the finally reduced spectrograms this can lead to ugly wiggling at wavelengths where the orders usually overlap and a loss of calibration at the very beginning and end.

CCD raw data should be subjected to a division by a flat field in order to account for sensitivity variations of various kinds on the chip. With CASPEC this is accomplished by illuminating the entrance slit of the spectrograph with either a built-in incandescent lamp or a bright screen attached to the dome. Dome flats necessitate very long exposure times, which is troublesome when one has to change the spectrograph settings often in a night. A well-known deficiency when using the incandescent lamp is that its light path through the optics is slightly different from the one taken by the stellar light. In the most general case this results in a small positional offset of the stellar and the flat field orders on the chip. For a proper pixel-by-pixel division the flat field orders should be appreciably wider than the stellar signal in order to ensure complete overlap by the flat. Otherwise, the stellar signal pixels would be divided by low or underexposed flat field pixels and give rise to spurious noise spikes in the output. Therefore, it is advisable to use a slit as long as possible for the flat without crowding the orders and choose the flat field exposure for the order tracing algorithms, rather than the stellar signal. Use of the stellar signal to trace the orders can be problematic if there are deep absorption lines in the spectrum. The fact that there is subtle, but not negligible, mechanical flexure in the spectrograph when moving the telescope from a program object to a standard star does not help. All these factors may cause the software slit to miss some fraction of the stellar signal, resulting in subsequent calibration problems. Finally, when the slit height is too small, there can be digital sampling errors as the software slit slants across the frame, leading to a few percent ripple in the measured total counts. These problems largely disappear if one is able to use a sufficient slit height, which can be done longward of 5000 Å where the interorder spacing is adequate.

Another effect to which close attention should be paid at all time during data reduction is that of scattered light in the spectrograph. This error source is particularly bothersome in the UV where its contribution is highest, and due to order crowding the standard countermeasures provided in MIDAS have the tendancy to either over or underestimate the background level. This correction affects absorption line depths or emission line heights in a direct way. There is no unequivocal recipe on how to proceed best. For example, we found that the deep absorption cores of the Ca II resonance

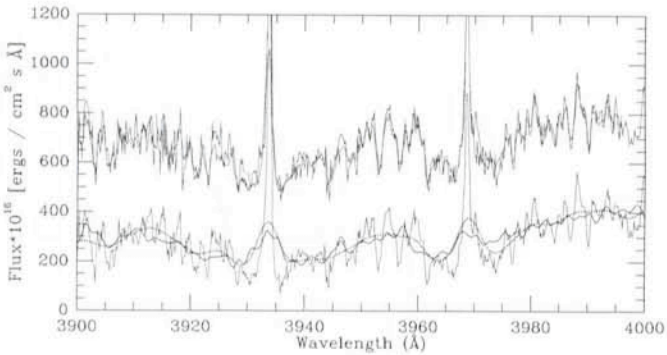

Fig. 1: *The flux calibration of the high resolution spectrograms was achieved by decreasing their resolution to the one of the (simultaneously obtained) photometric IDS spectra and a subsequent multiplication by the smoothed ratio of both signals. The figure shows (a) 5 individually calibrated orders, (b) the merged section of the echelle spectrogram (thin line), (c) this section after a convolution with a FWHM = 4.5 Å gaussian (dots), and (d) the original IDS spectrogram (fat line) of Sz06.*

lines had negative counts after treatment with MIDAS. This is due to an overestimation of the true background because of the order crowding. A more detailed study of individual frames is likely to be necessary in cases like this. Concerned readers may want to study the treatment of this problem elsewhere (c.f. the literature available on IUE high resolution data reduction).

In order to assign flux levels to the individual echelle orders we directly utilized the simultaneously obtained photometric IDS spectra. For calibration the resolution of the CASPEC spectrograms had to be decreased to that of the IDS. The values of 12,000 and 500/1 000 quoted above were obtained by evaluating the FWHM of the autocorrelation function of a comparison spectrogram. A convolution of the IDS data with gaussian functions of FWHM of 4.5 Å and 14 Å gave satisfactory results, although the instrumental profile of the IDS is not a strict gaussian. The flux correction is then the ratio of the smoothed echelle and unsmoothed IDS spectrogram. This generally well behaved function was approximated by a spline which disregarded high frequency noise in the IDS data. The echelle orders were then merged, using a full linear ramp length of 14 pixels at the edges and equal weights elsewhere. Fig. 1 gives an example of the procedure, showing (a) 5 individually calibrated orders, (b) the merged section of the echelle spectrogram, (c) this section after a convolution with a FWHM = 4.5 Å gaussian, and (d) the original IDS spectrogram. Note how well individual orders reproduce in the overlapping region. The final absolute accuracy of the photometric data is estimated by various cross checks with different flux standards to be on the order of 4–6 % over the whole range, and with relative errors within short wavelength intervals even smaller.

The RCA chip used for CASPEC shows fairly uniform quantum efficiency and only a very small fringing effect below 4 000 Å. Under these nearly ideal conditions one can work on frames using all the techniques mentioned above but without applying a flat field division. A quantitative comparison has shown that in the UV the final result was little affected by either using a flatfielded or a non-flatfielded frame.

Chapter IV

The White Queen whispered: "And I'll tell you a secret – I can read words of one letter! Isn't that grand? However, don't be discouraged. You'll come to it in time."

Due to the extremely high information content of the material obtained, our contribution at this time can be nothing more than an inadequate outline of a few empirical approaches we have taken so far. Because of the vast amount of work possible we are forced to initially emphasize certain approaches and targets. Thus, we are currently performing a case study with the stars Sz06 and Sz68, which are identical in most parameters (spectral type both K2, $L_\odot$ 2.3 vs. 2.8, v sini 34 vs. 42 km/s, W_λ (LiI6707) 0.43 vs. 0.42 Å), except for activity levels ($W_\lambda(H\alpha)$ –35.2 vs. –4.4 Å, and values of R_K whose ratio is 1.9). The star Sz19 of spectral type G2 is an ideal object to compare the detailed knowledge available for the sun to the T Tauri regime and is also receiving special attention. Far more interpretation is in progress and will be reported later. However, we would like to comment on a number of interesting results already available.

Values of v sini for the target stars can be obtained by either using Fourier, autocorrelation or direct matching techniques (c.f. Gray 1976). The available sampling step and S/N allows the detection of the characteristic zeros in the power spectra down to a lower limit of v sini = 14 km/s. Bouvier and Bertout (1985) have already given an outline of one method for applying these procedures to T Tauri stars. We were able to actually see the zeros directly by taking power spectra of various segments of the full merged echelle spectra and averaging these power spectra. The main advantage of the averaging is to greatly reduce what is referred to as "beating". (One should also bear in mind that the characteristic zeros are wavelength dependent, since v sini = $(.660 \times c) \div (\lambda \times \sigma_1)$, where σ_1 is the frequency of the first zero.) Very consistent results were obtained from the autocorrelation and direct matching determinations.

Our main interest centers on line ratios and absolute line and continuum fluxes. The approach to study the chromospheric structure is to consider the flux ratio of T Tauri stars relative to standard stars after the latter have been convolved with a proper rotational function (c.f. Strom 1983). Any chromospheric activity will then show up as excessive emission, related to particular lines. Because our material is calibrated, we can determine both general brightening of the UV continuum after dereddening and the enhanced emission in particular lines. The material can also be compared directly with spatially resolved spectroscopy of solar plages (e.g. LaBonte 1985).

Of course, both object and standard have to be moved to the same reference wavelength system; namely that of the stellar photosphere. Unfortunately, the resulting wavelength shift also affects the ever-present telluric lines, which already are in the same frame (and there are far more water lines at R = 12,000 than we ever dreamt of). Ideally, those lines should be removed *ab initio*, but this is rather hard to accomplish. As a result, virtual features can appear in the ratio plots. We have considered whether to present differences or ratios. The difference plots are only meaningful when made between spectra with continua normalized to the same value. Spectra in this form were made for the red frames. In the UV it is increasingly difficult to determine the true continuum, so we present ratios. Comparison between ratio and difference representations of the red data show no qualitative differences.

The first striking point to be seen in looking at the ratio plots (Fig. 2) is the high degree to which the weak and medium strength photospheric lines divide out. This gives us confidence that all the reduction stages have worked relatively well. Only the stronger absorption features in the standard star appear to fill up in the T Tauri stars. This phenomenon is easily seen the UV and infrared lines of neutral and ionized calcium, the Balmer lines, the sodium doublet, and a number of iron

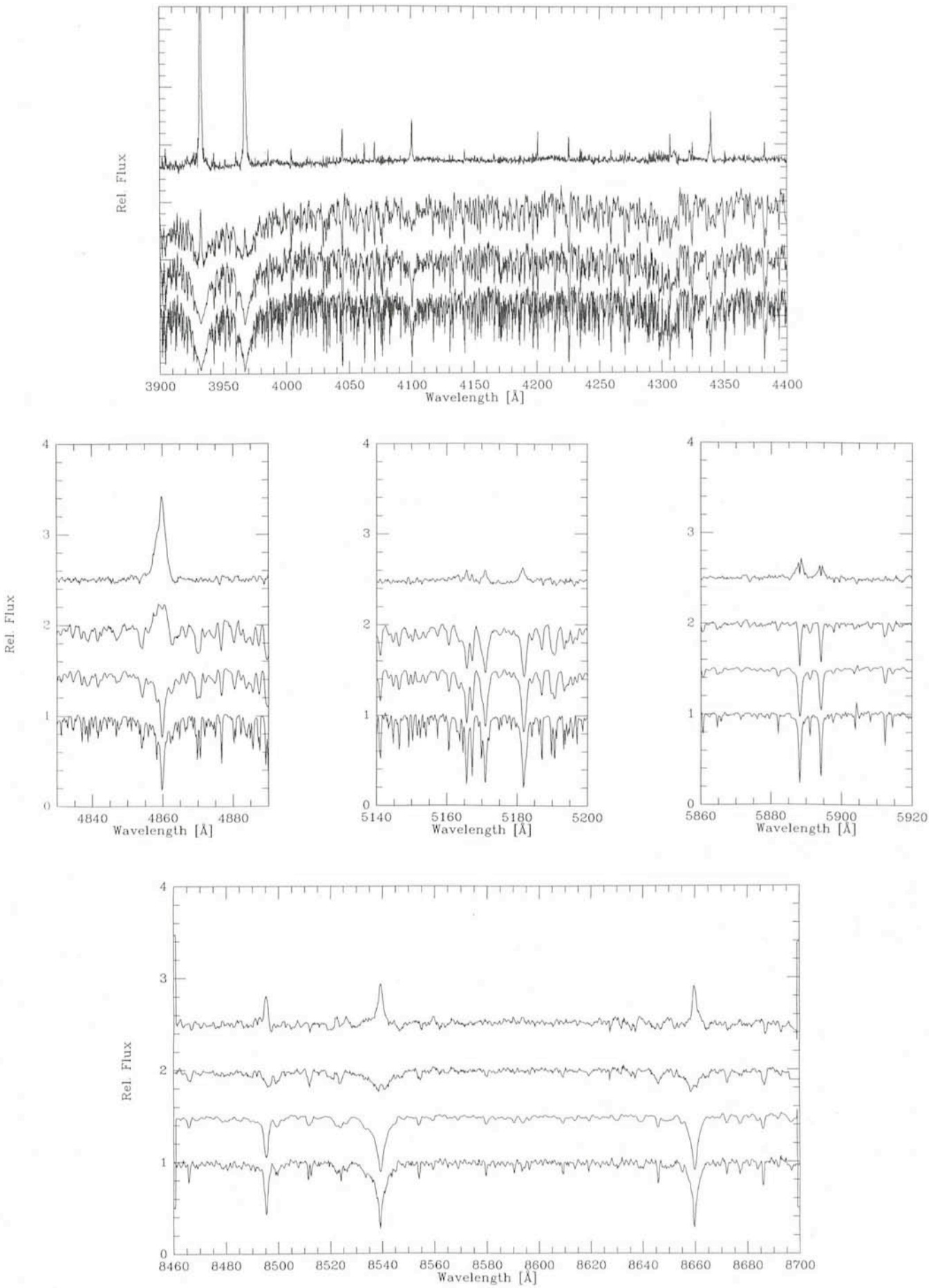

Fig. 2: *Illustration of excessive emission for Sz19 in the UV (a); at H_β, Mg I B, and N a D (b); and at the IR triplet (c). The figures give (from bottom to top) a spectroscopic standard (1); the standard convolved with a rotational function of v sini = 30 km/s (2); Sz19 (3); and the ratio (3):(2). Note that the two residual components of N a D obey a flux ratio of 2.0, and indicate the presence of an interstellar absorption feature, too.*

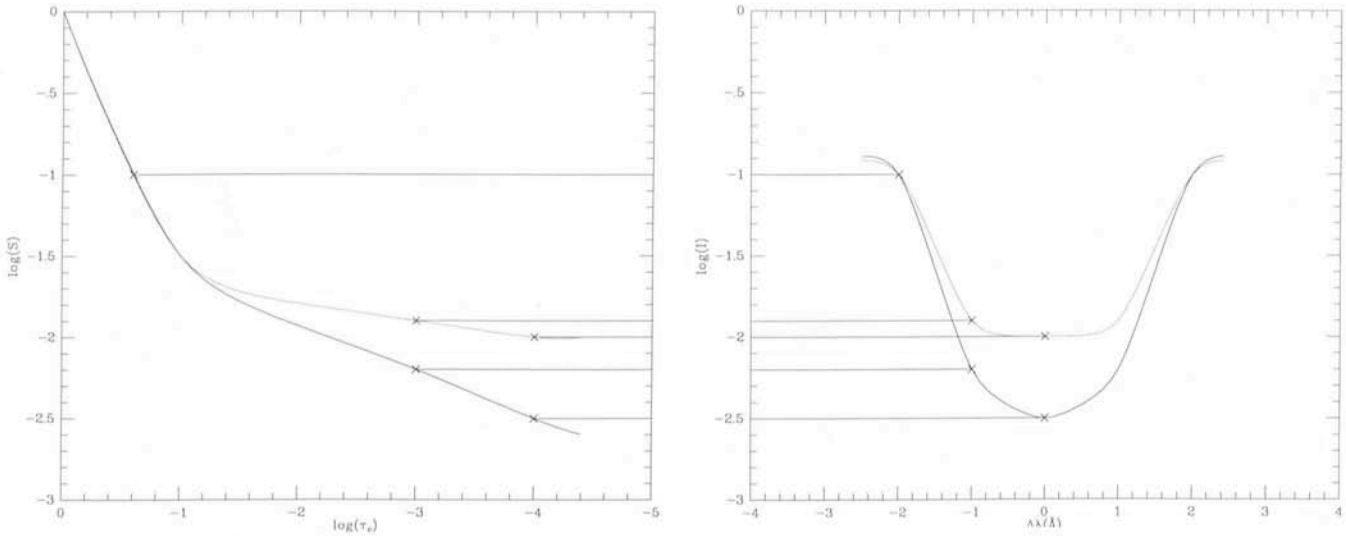

Fig. 3: *A schematic representation of the Eddington-Barbier relation in a spectral line and how an atmospheric perturbation can give rise to an emission feature in the ratio plots of Fig. 2. On the left are LTE source functions for a quiet (lower) and active (upper) star, with various line optical depth points marked. The way these translate to the line profile is shown on the right; the active star yields a brighter line core which appears as a positive ratio feature. The situation in a real star has a number of additional complications.*

lines. It is not caused by too low a zero level in the T Tauri UV spectra, since there are cases of lines with equal strength in the standard spectra of which only some appear as emission features in the ratio spectra (e.g. 4215 Å). The same effect is also seen in the red frames for which there is no question about the zero level. The stronger features are even apparent in the IDS spectra at much lower resolution. It is gratifying to note that the ratio spectra bear a close resemblance to solar chromospheric limb spectra. The lines which show up are those expected to be formed above the deep photosphere in the stellar atmosphere.

The qualitative explanation of this behaviour is straightforward: since the strong absorption lines probe a region further away from the stellar surface, this effect is presumably due to a differential increase of the source function at a given optical depth. Suppose one were to overlay a plot of the source function against optical depth (see Fig. 3) for a standard star and a T Tauri star (assuming that all lines share the same depth dependent source function, i.e. LTE). Then, for example, the residual intensity at the core of each line should reflect the value of this source function at approximately unit line center optical depth in each line. If we suppose the T Tauri star is identical to the standard star deep in the photosphere, and that its source function becomes increasingly larger as we move outward above a certain depth, then lines which become optically thick below that point will look the same in both stars, while lines formed above that point should have brighter cores in the T Tauri star. Thus, the depth of formation of lines which just begin to show up in the ratio plot is the depth at which the atmosphere of the T Tauri star is significantly perturbed relative to its main sequence counterpart. The fact that the weak lines are absent in the observed ratio spectra is proof that if you look deeply enough into a T Tauri star it looks "normal". By studying the excess emission as a function of depth, one obtains quantitative measures of the non-radiative heating structure of the atmosphere. Comparison of ratio plots for different stars gives an immediate useful characterization of the activity levels. Of course the real situation is not nearly as simple as outlined above; in the end one must take the presence of a feature in the ratio plot as a guide that detailed physical analysis of that line will be profitable. One must also keep in mind the possible circumstellar contributions especially in the very strong lines.

Ultimately, our purpose is to apply the full NLTE treatment of semi-empirical modeling to the data. We have, for example, calibrated line profiles for the Ca I, II resonance lines and Ca II IR triplet obtained at the same time. A model atmosphere which produces the desired synthetic profiles for these diagnostics can then be tested for consistency with the Balmer, Na D, Mg I B, etc. lines. Each line contributes a unique set of constraints to the emerging model. The model should also be able to explain the ratio spectrum and any UV continuum excess. We can hope to separate the near surface and circumstellar contributions to the spectrum and understand each with such detailed analysis. In the process, we will understand the relation of the pre-main sequence activity to its main sequence counterpart, and bring the level of ignorance about T Tauri stars to that for more studied examples of stellar activity.

References

Appenzeller, I., Jankovics, I., Krautter, J. 1983, *Astron. Astrophys. Suppl.* **53,** 291.

Baldwin, J. A., Stone, R.P.S. 1984, *M.N.R.A.S.* **206,** 241.

Bouvier, J., Bertout, C. 1985, *The Messenger* **39,** 33.

Carroll, L. MDCCCLXXI, Through the Looking-Glass and What Alice Found There, Macmillan.

Gray, D.F. 1976, The Observation and Analysis of Stellar Photospheres, Wiley, Toronto.

LaBonte, B.J. 1985, *Astrophys. J.,* preprint.

Schwartz, R.D. 1977, *Astrophys. J. Suppl.* **35,** 161.

Strom, S.E. 1983, *Revista Mex. Astron. Astrof.* **7,** 201.

List of ESO Publications

The following publications are still available:

Conference on "The Role of Schmidt Telescopes in Astronomy", Hamburg 21–23 March 1972. Proceedings. Ed. U. Haug. 160 p. DM 16.–

ESO/SRC/CERN Conference on "Research Programmes for the New Large Telescopes", Geneva, 27–31 May 1974. Proceedings. Ed. A. Reiz. 398 p. ISBN 3-923524-02-1. DM 40.–

ESA/ESO Workshop on "Astronomical Uses of the Space Telescope", Geneva, 12–14 February 1979. Proceedings. Eds. F. Macchetto, F. Pacini and M. Tarenghi. 408 p. ISBN 3-923524-06-4. DM 40.–

"Dwarf Galaxies", Proceedings of the First ESO/ESA Workshop on the Need for Coordinated Space and Ground-based Observations. Geneva, 12–13 May 1980. Eds. M. Tarenghi and K. Kjär. 186 p. ISBN 3-923524-09-9. DM 10.–

ESO Workshop on "Two Dimensional Photometry", Noordwijkerhout, 21–23 November 1979. Proceedings. Eds. P. Crane and K. Kjär. 412 p. ISBN 3-923524-07-2. DM 40.–

ESO Conference on "Scientific Importance of High Angular Resolution at Infrared and Optical Wavelengths". Garching, 24–27 March 1981. Proceedings. Eds. M.-H. Ulrich and K. Kjär. 444 p. ISBN 3-923524-10-2. DM 50.–

ESO Workshop on "The Most Massive Stars". Garching, 23–25 November 1981. Proceedings. Eds. S. D'Odorico, D. Baade and K. Kjär. 366 p. ISBN 3-923524-11-0. DM 50.–

"The ESO/Uppsala Survey of the ESO (B) Atlas". Ed. A. Lauberts. 1982. 504 p. ISBN 3-923524-13-7. DM 40.–

"Evolution in the Universe". Symposium held on the occasion of the inauguration of the ESO Headquarters building in Garching on 5 May 1981. With contributions by H. Curien, H. Alfvén, M. Eigen, L. Van Hove, J. H. Oort and D. W. Sciama. 122 p. ISBN 3-923524-12-9. DM 20.–

ESO Workshop on "The Need for Coordinated Ground-based Observations of Halley's Comet". Paris, 29–30 April 1982. Proceedings. Eds. P. Véron, M. Festou and K. Kjär. 310 p. ISBN 3-923524-14-5. DM 35.–

"Second ESO Infrared Workshop". Garching, 20–23 April 1982. Proceedings. Eds. A.F.M. Moorwood and K. Kjär. 446 p. ISBN 3-923524-15-3. DM 50.–

ESO Workshop on "Primordial Helium". Garching, 2–3 February 1983. Proceedings. Eds. P.A. Shaver, D. Kunth and K. Kjär. 422 p. ISBN 3-923524-16-1. DM 50.–

Workshop on "ESO's Very Large Telescope". Cargèse, 16–19 May 1983. Proceedings. Eds. J.-P. Swings and K. Kjär. 270 p. ISBN 3-923524-17-X. DM 40.–

ESO Workshop on "Site Testing for Future Large Telescopes". La Silla, 4–6 October 1983. Proceedings. Eds. A. Ardeberg and L. Woltjer. 207 p. ISBN 3-923524-18-8. DM 25.–

First ESO-CERN Symposium "Large-Scale Structure of the Universe, Cosmology and Fundamental Physics". Geneva, 21–25 November 1983. Proceedings. Eds. G. Setti and L. Van Hove. 455 p. DM 35.–

IAU Colloquium No. 79 "Very Large Telescopes, their Instrumentation and Programs". Garching, 9–12 April 1984. Proceedings. Eds. M.-H. Ulrich and K. Kjär. 908 p. ISBN 3-923524-19-6. DM 80.–

ESO Workshop on "The Virgo Cluster of Galaxies". Garching, 4–7 September 1984. Proceedings. Eds. O.-G. Richter and B. Binggeli. 477 p. ISBN 3-923524-20-X. DM 50.–

ESO Workshop on "Production and Distribution of C, N, O Elements". Garching, 13–15 May 1985. Proceedings. Eds. I.J. Danziger, F. Matteucci and K. Kjär. 429 p. ISBN 3-923524-21-8. DM 50.–

ESO-IRAM-Onsala Workshop on "(Sub)Millimeter Astronomy". Aspenäs, Sweden, 17–20 June 1985. Proceedings. Eds. P. A. Shaver and K. Kjär. 644 p. ISBN 3-923524-22-6. DM 70.–

Payment has to be made in advance (preferably by cheque) to the European Southern Observatory, Financial Services, Karl-Schwarzschild-Str. 2, D-8046 Garching bei München, or to the ESO bank account No. 2102002 with Commerzbank München.

First IRSPEC Spectra

Following a successful first test on the 3.6 m telescope it is now expected that IRSPEC will be available for Visiting Astronomers in Period 38. This instrument is a cooled grating infrared spectrometer capable of achieving a maximum resolving power of 2.10^3 with a 6×6 arcsecond entrance aperture. It is currently equipped with a 32 element array detector sensitive between 1 μm and 5 μm, and any desired spectral region within this range can be covered by stepping the grating under computer control. As the test only ended in early December it is too early to provide detailed performance figures here. These will be made available via a formal announcement and/or more extensive article in the *Messenger* before the April proposal deadline. In the meantime however, the two accompanying spectra illustrate the type of spectrum display available on-line at the telescope.

A. MOORWOOD

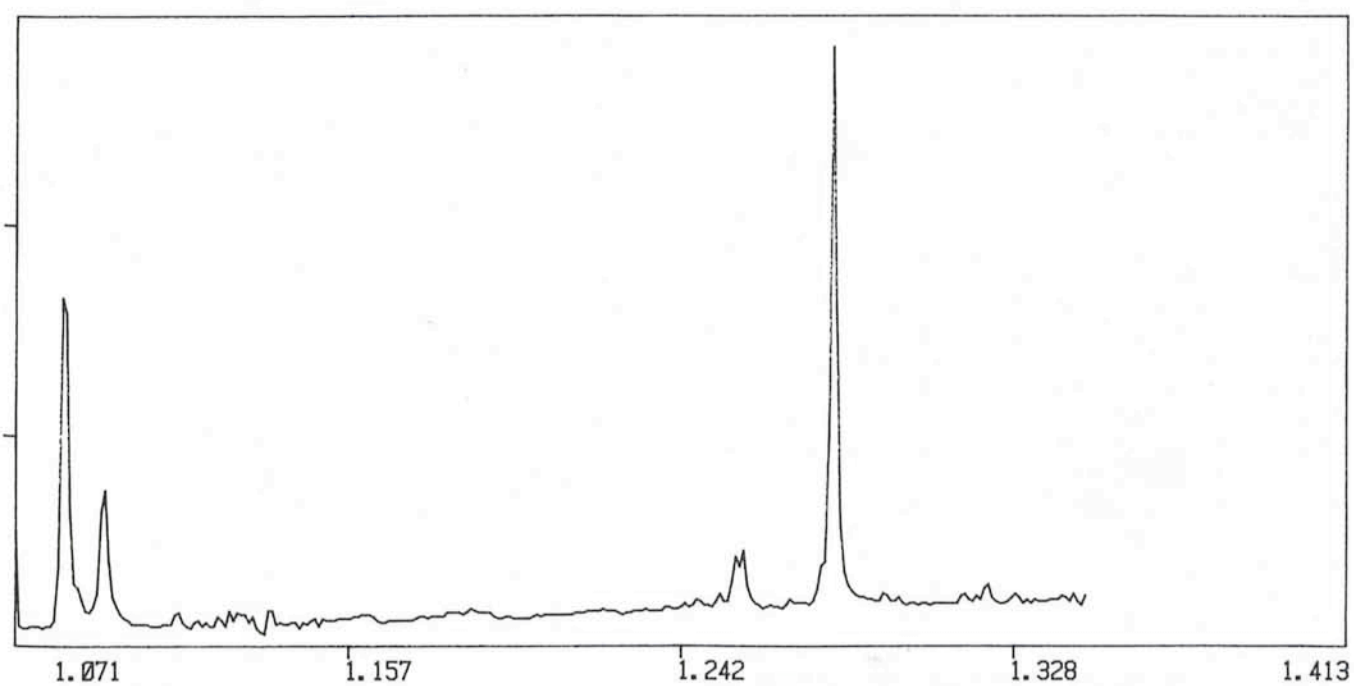

Fig. 1: *ηCar/standard star. Wavelength scale is in microns. "Noise" around 1.1 μm is due to imperfectly cancelled atmospheric absorption.*

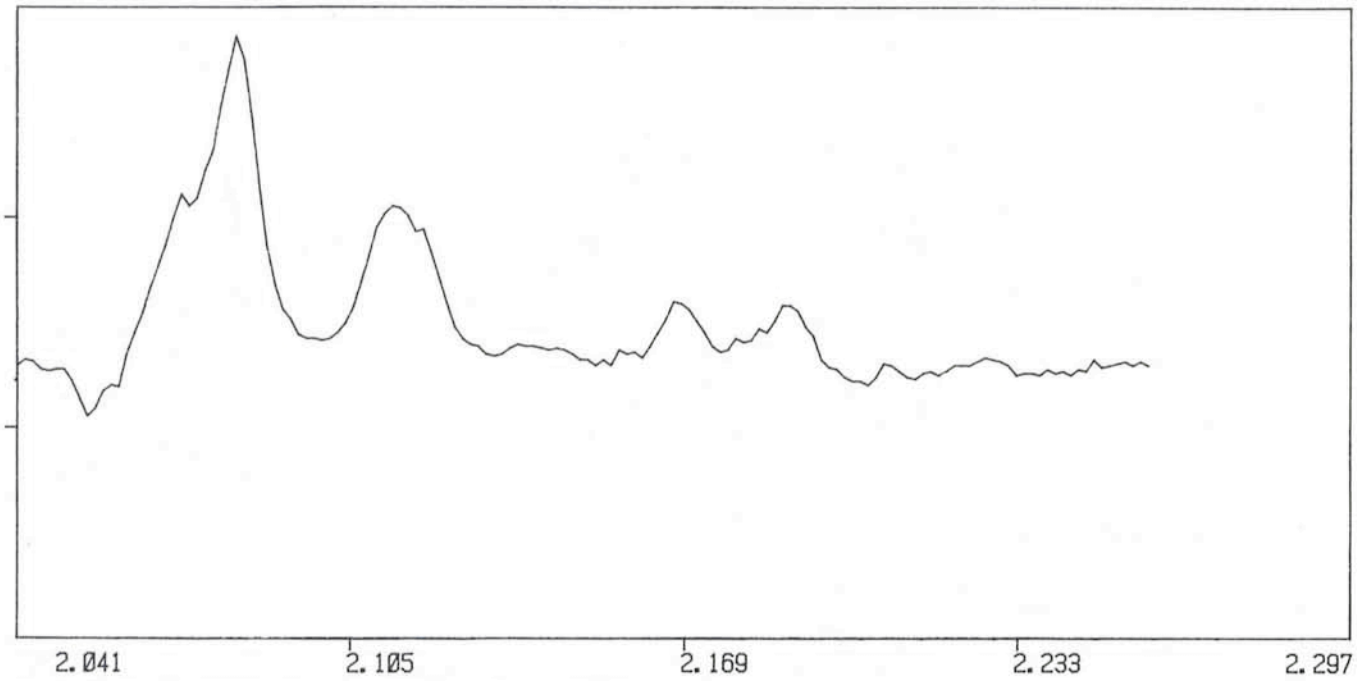

Fig. 2: γ^2 *Velorum/standard star. Wavelength scale is in microns.*

Comet Halley Observed at ESO

Comet Halley was photographed with the ESO 1 metre Schmidt telescope at La Silla on December 9, 1985. The exposure was 10 minutes on a blue-sensitive emulsion. The telescope was guided on the moving comet. The stars in the field are therefore seen as short trails.

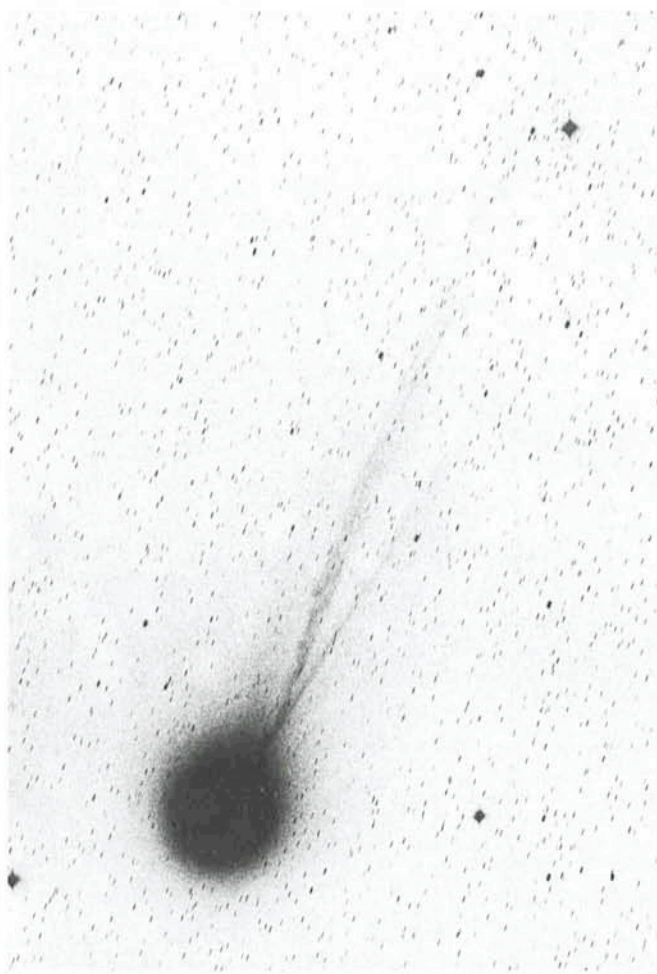

Comet Halley photographed with the ESO 1 m Schmidt telescope on December 9, 1985. Scale of the photograph: 1 degree = ~ 5 cm.

Although Comet Halley is somewhat brighter (magnitude 4 on December 12) than originally predicted, it has been slow in developing a tail. This negative picture, which has been somewhat enhanced for clarity, shows two tails pointed towards East (away from the Sun). The thin, very straight tail (the northernmost) is a typical ion-tail, consisting of charged particles, which are pushed away from the comet by the solar wind (charged particles travelling away from the Sun at high speeds). The other ion tail, which is slightly bent and broader, can be followed to a distance of about 2.5 degrees (more than 5 million kilometres) from the comet's head. The bend ("kink") is due to a change in the solar wind direction. Both tails are enveloped in a very faint cloud of dust particles, also released from the comet.

When the picture was taken, Comet Halley was about 200 million kilometres from the Sun and 110 million kilometres from the Earth. It is moving south in the sky and is becoming more and more difficult to view from Europe. In early February, it disappears from view, when it passes behind the Sun. It is expected that it can be seen again around February 15.

Many of the ESO telescopes will be used for observations of Comet Halley during early 1986.

El cometa Halley observado en la ESO

El día 9 de diciembre de 1985 se tomó una fotografía del cometa Halley con el telescopio Schmidt de 1 m. La exposición fue de 10 minutos. El telescopio fue dirigido en dirección del cometa en movimiento, y por lo tanto las estrellas aparecen como rayas cortas.

Cuando se tomó la fotografía el cometa Halley se encontraba a una distancia de aproximadamente 200 millones de kilómetros del sol y a 110 millones de kilómetros de la tierra. A principios de febrero pasará por detrás del sol y desaparecerá de la vista. Se espera que volverá a verse alrededor del 15 de febrero.

Se usarán varios telescopios de la ESO para hacer observaciones del cometa Halley a principios del año 1986.

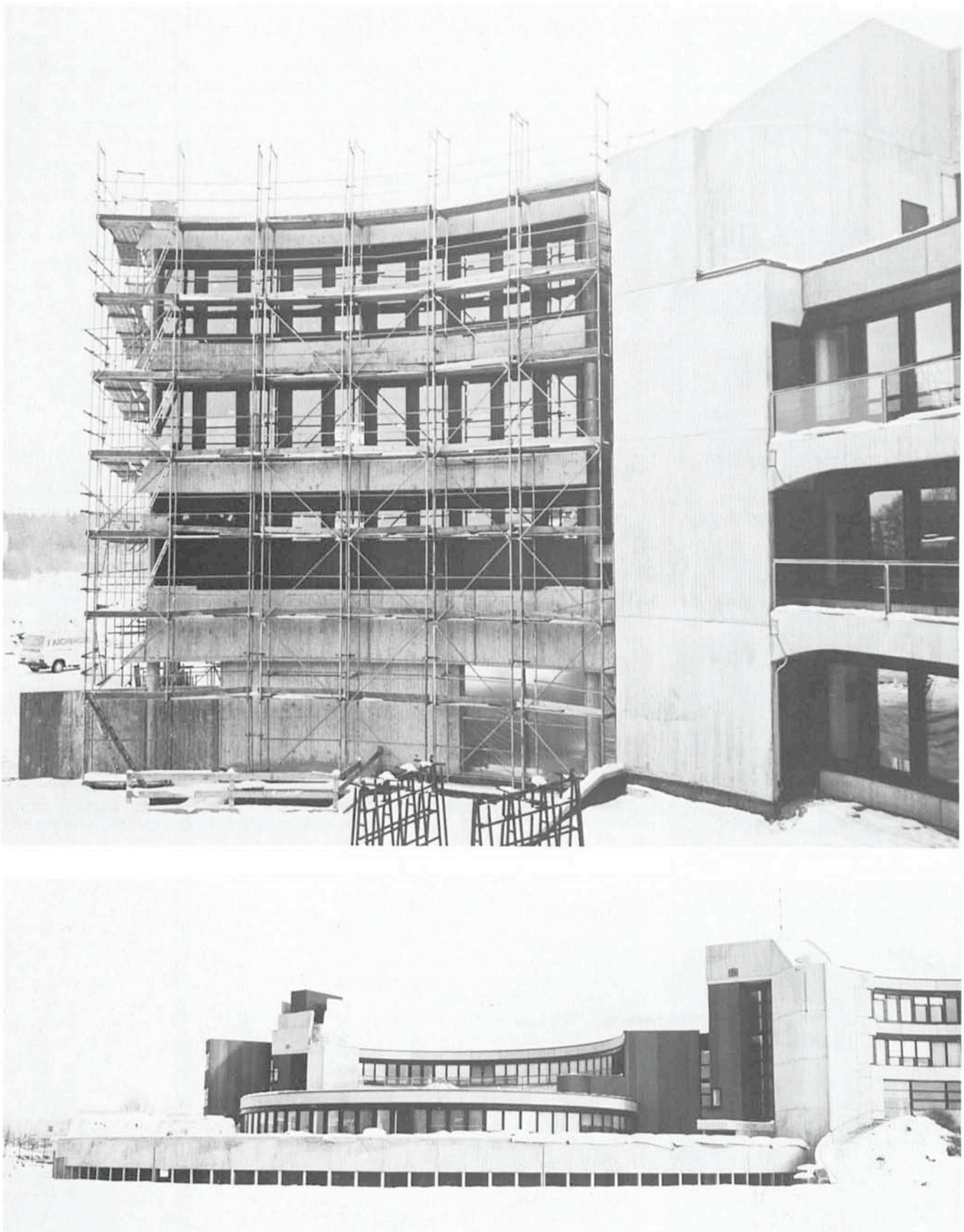

The extensions of the ESO Headquarters building in Garching photographed end of November 1985. The rough construction work is now completed and work on the technical installations is in progress. The upper picture shows the new north-east wing where space for computers, offices and a conference room will become available next spring. The picture below shows the extension of the workshop and laboratory area.

Estas fotografías que fueron tomadas hacia fines de Noviembre de 1985 muestran las ampliaciones del edificio principal de la ESO en Garching. La obra gruesa está terminada y ahora están progresando los trabajos de las instalaciones técnicas. La fotografía de arriba muestra el ala noroeste donde se instalarán las computadoras, oficinas y una sala de conferencia que estarán a disposición a partir de la próxima primavera. La fotografía en la parte inferior muestra la ampliación de los talleres y laboratorios.

ESO, the European Southern Observatory, was created in 1962 to . . . establish and operate an astronomical observatory in the southern hemisphere, equipped with powerful instruments, with the aim of furthering and organizing collaboration in astronomy . . . It is supported by eight countries: Belgium, Denmark, France, the Federal Republic of Germany, Italy, the Netherlands, Sweden and Switzerland. It operates the La Silla observatory in the Atacama desert, 600 km north of Santiago de Chile, at 2,400 m altitude, where thirteen telescopes with apertures up to 3.6 m are presently in operation. The astronomical observations on La Silla are carried out by visiting astronomers – mainly from the member countries – and, to some extent, by ESO staff astronomers, often in collaboration with the former. The ESO Headquarters in Europe are located in Garching, near Munich.
ESO has about 135 international staff members in Europe and Chile and about 120 local staff members in Santiago and on La Silla. In addition, there are a number of fellows and scientific associates.

The ESO MESSENGER is published four times a year: in March, June, September and December. It is distributed free to ESO personnel and others interested in astronomy.
The text of any article may be reprinted if credit is given to ESO. Copies of most illustrations are available to editors without charge.

Technical editor: Kurt Kjär

EUROPEAN
SOUTHERN OBSERVATORY
Karl-Schwarzschild-Str. 2
D-8046 Garching b. München
Fed. Rep. of Germany
Tel. (089) 32006-0
Telex 5-28282-0 eo d
Telefax: (089) 3202362

Printed by Universitätsdruckerei
Dr. C. Wolf & Sohn
Heidemannstraße 166
8000 München 45
Fed. Rep. of Germany

ISSN 0722-6691

FRANK MIDDELBURG 1936–1985

La noticia de la desaparición de Frank Middelburg, en el día 15 de Noviembre de 1985, conmovió a todo el mundo astronómico con un sentimiento especial de tristeza. Frank no sólo era un experto reconocido en el campo de procesamiento de imagen y un ingeniero de sistemas altamente respetado, también era un preciado amigo y colega.

Nacido en Hong Kong, el 8 de Octubre de 1936, hijo de un embajador, Frank estuvo desde el principio relacionado con un ambiente internacional. Poco después de casarse con Anita, ingresó en ESO en 1967 como uno de los primeros funcionarios europeos en Chile. La experiencia que ganó en La Silla, primero en meteorologia y después como observador, fue de gran valor para su posterior carrera.

Cuando los primeros ordenadores llegaron a ESO-Chile, Frank se convirtió en el primer experto local de *software*. Llegó a conocer en profundidad, rápidamente, no sólo los ordenadores, sino también las técnicas de procesado de imagen, en ese tiempo virtualmente desconocidas. Fue como experto en procesado de imagen que dejó Chile para trabajar en las oficinas centrales de ESO, primero en Ginebra, luego en Garching.

Desde el principio de los setenta, las técnicas de *software*, optimizadas para la reducción y análisis de objetos celestes, han sido de importancia crucial en el desarrollo explosivo de la Astrofísica. En todo el mundo, grupos de especialistas han dedicado gran cantidad de tiempo y esfuerzo a mejorar estas técnicas.

Frank lo hizo todo solo. Con una magnífica comprensión de las prioridades, diseñó un sistema de *software* poderoso y versátil con especial énfasis en imágenes espectrales. Los resultados de los esfuerzos de Frank fueron realmente impresionantes. Su Programa de Tratamiento de Imágenes (IHAP) no tiene todavía rival en el análisis de observaciones de espectroscopía estelar. Al mismo tiempo, mientras aparecían y desaparecían otros sistemas de procesamiento de imagen, Frank mejoró progresivamente el potencial de su IHAP. Fue una muestra de su éxito el que recibiera tantas solicitudes de institutos e individuos para resolver sus problemas, a menudo muy especiales. Una prueba de la capacidad y habilidad de Frank, así como de su generosidad, fue el hecho de que, a pesar de todo, resolvió virtualmente todos esos problemas.

Hoy en día, unos 15 importantes institutos tienen instalado IHAP. Muchos mas sueñan con tenerlo, sueños impedidos por incompatibilidades de electrónica. Actualmente, la diseminación de las posibilidades de IHAP se acelera a través de su incorporación en el sistema MIDAS de ESO.

Es difícil sobreestimar la importancia de la contribución de Frank en la producción europea de datos espectrográficos astronómicos. Una gran parte de los principales científicos han dependido, y aun dependen, de la obra de un solitario diseñador de *software*, utilizando IHAP para convertir sus observaciones en datos interpretables físicamente.

Aquellos de nosotros que compartimos el privilegio de unos profundos lazos de amistad con la familia de Frank, también compartimos un recuerdo común de la inspiradora atmósfera típica de su hogar. Recordaremos siempre nuestras discusiones sobre literatura, arte, música, política y otros temas tratados en la forma especial de Frank Middelburg. Nuestra profunda simpatía a Anita, Saskia y Miriam, que dieron a nuestro amigo Frank el apoyo en sus últimos y difíciles años. Sabiendo lo poco que podemos hacer para consolarles en esta gran pérdida, podemos sólo asegurarles que la memoria de Frank estará para siempre con nosotros.

A. ARDEBERG

Contents